



# Local Features: From SIFT to Differentiable Methods



Vasileios Balntas  
Facebook Reality Labs



Dmytro Mishkin  
Czech Technical  
University



Edgar Riba  
Computer Vision Center

# Tutorial Programme Overview

Classical  
& modern  
methods



From paper to  
practice

## Image Matching Across Wide Baselines: From Paper to Practice

Yihei Jin · Dmytro Mishkin · Anastasiia Mishchuk · Jiri Matas · Pascal Fua ·  
Kwong Moo Yi · Eduard Trulls

Received: date / Accepted: date

**Abstract** We introduce a comprehensive benchmark for local features and robust estimation algorithms, focusing on the downstream task – the accuracy of the reconstructed camera pose – as our primary metric. Our pipeline’s modular structure allows us to easily integrate, compile, and combine different methods and heuristics. We demonstrate this by embedding dozens of popular algorithms and evaluating them, from seminal works to the cutting edge of machine learning research. We show that with proper settings, classical solutions may still outperform the *perceived* state of the art.

Besides establishing the *actual* state of the art, the experiments conducted in this paper reveal unexpected properties of Structure from Motion (SfM) pipelines that can

This work was partially supported by the Natural Sciences and Engineering Research Council of Canada (NSERC) Discovery Grant “Deep Visual Geometry Machines” (R0PNS-2018-07768), by systems supplied by Cloupoint Canada, and by Google’s Visual Positioning Service. DM and JM were supported by EP VVV funded project CZJ22 (018/00/016 019/0000765 “Research Center for Informatics”). DM was also supported by CTV student grant S0517155P0K37711 and by the Austrian Ministry for Research, Innovation and Technology, the Federal Ministry for Digital and Economic Affairs, and the Province of Upper Austria in the frame of the COMET center SCCH. JM was supported by the Swiss National Science Foundation.

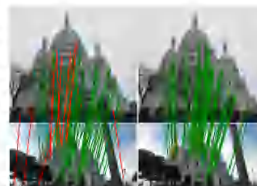


**Fig. 1** Every paper claims to outperform the state of the art. Is this possible, or an artifact of insufficient validation? On the left, we show, stem matches extracted with D2-Net [70] (v1), a state-of-the-art local feature, using OpenCV RANSAC with its default settings. We code the outliers in green if they are correct and red otherwise. On the right, we show SIFT [60] (v3) with a carefully tuned MAGSAC [15] – notice how the latter performs much better. This illustrates our take-home message: to correctly evaluate a method’s performance, it needs to be embedded within the pipeline used to solve a given problem, and the different components in said pipeline need to be tuned carefully and jointly, which requires engineering and domain expertise. We fill this need with a new, modular benchmark for sparse image matching, incorporating details of built-in methods.

Kornia  
library



# kornia

# Programme

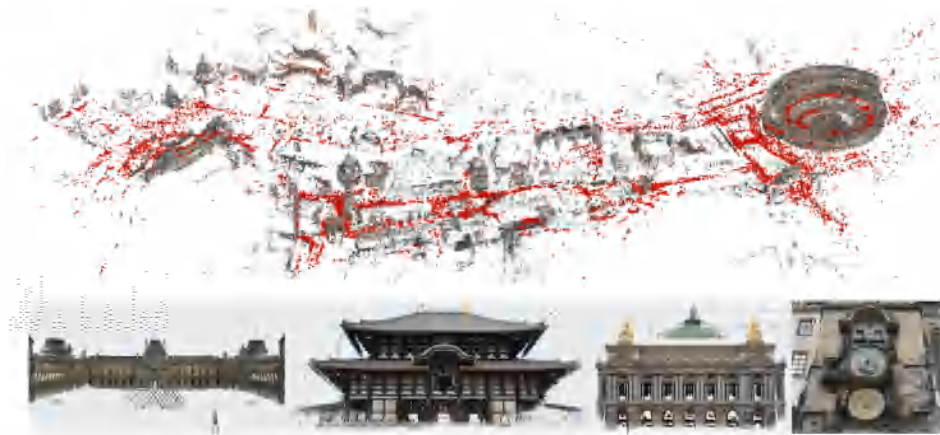
- 09:00 – 10:00 Overview of classical & end-to-end methods
- 10:00 – 11:00 Local features: from paper to practice
- 11:00 – 12:00 Kornia introduction & hands-on Session

<https://local-features-tutorial.github.io/>

# What is image matching?



# Why is image matching useful?



SfM

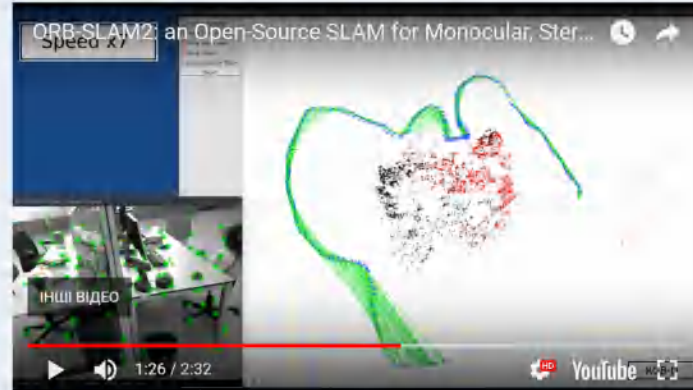
L. Schonberger and J.-M. Frahm,  
**Structure-from-Motion Revisited**, 2016  
COLMAP

# Why is image matching useful?

## ORB-SLAM2 for Monocular, Stereo and RGB-D Cameras

Code: [https://github.com/raulmur/ORB\\_SLAM2](https://github.com/raulmur/ORB_SLAM2).

Paper: Raúl Mur-Artal, and Juan D. Tardós. ORB-SLAM2: an Open-Source SLAM System for Monocular, Stereo and RGB-D Cameras. ArXiv preprint [arXiv:1610.06475](https://arxiv.org/abs/1610.06475), 2016



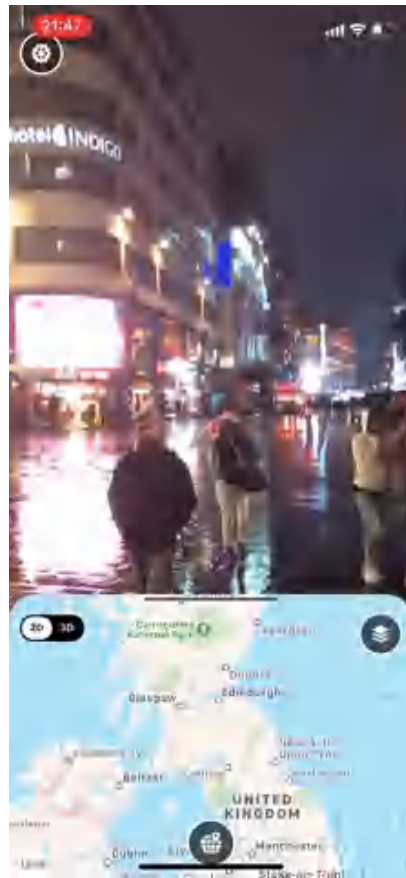
SLAM

R. Mur-Artal, and J. D. Tardós.

**ORB-SLAM2: an Open-Source SLAM System for  
Monocular, Stereo and RGB-D Cameras**, arXiv 2016



# Localisation



SCAPE

# Why is image matching useful?

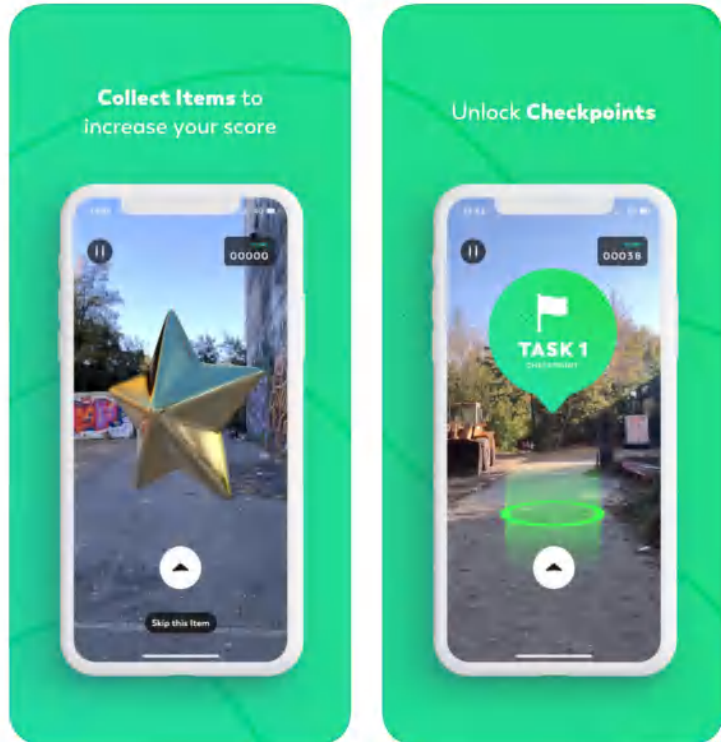


SLAM

Daniel DeTone, Tomasz Malisiewicz, Andrew  
Rabinovich, Superpoint.  
**MagicLeap SLAM**



# Why is image matching useful?



Augmented Reality  
**ScavengAR** App

# Why is image matching useful?

## Panoramas

Brown and Lowe, **Automatic panoramic image stitching using invariant image features**

Image: Rick Szeliski



(a) Image 1



(b) Image 2



(c) SIFT matches 1



(d) SIFT matches 2



(e) RANSAC inliers 1



(f) RANSAC inliers 2



# Image Matching - Practicality

- Matching a set of images enables us to “recover” the geometry of the world from individual images.
- To understand why, we need to quickly discuss a few things about cameras.

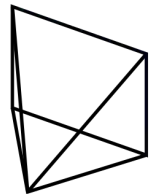
Scene B



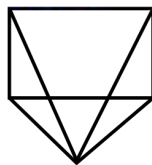
Scene A



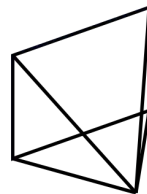
Scene C



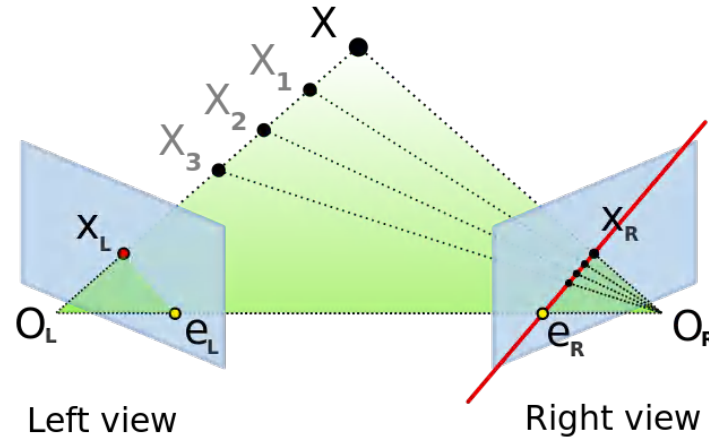
*Camera Motion*<sub>A→B</sub>



*Camera Motion*<sub>A→C</sub>



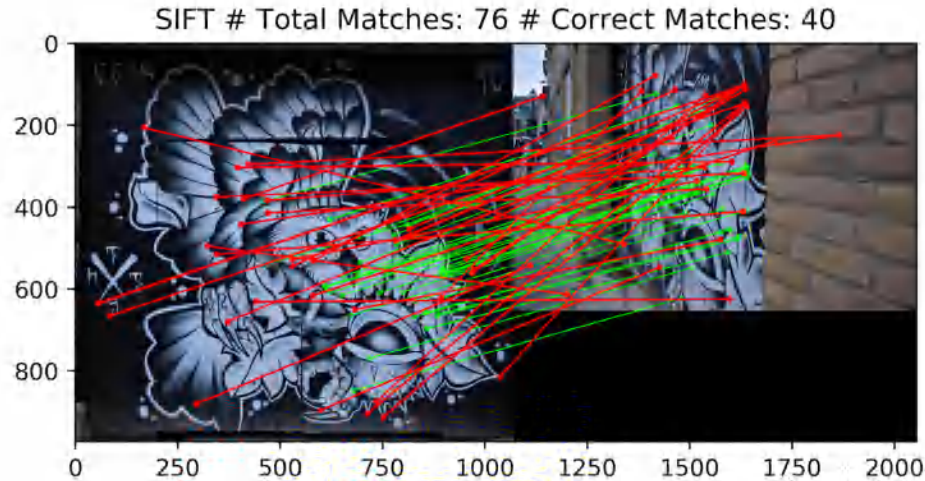
## Point correspondences for triangulation



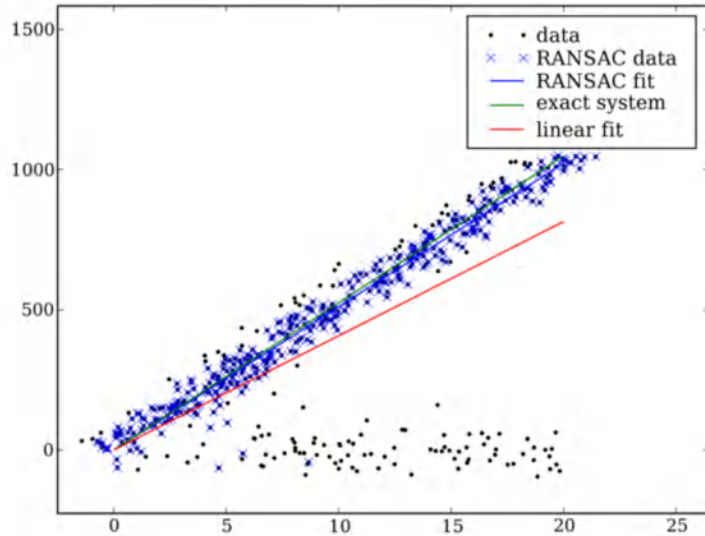
- One left-view to right-view match is not enough
- Min number of matches defined by theory and algorithms (e.g. 8-point algorithm)
- Practically we aim for a higher number of matches than the theoretical (e.g.  $> 100$ )

<sup>1</sup>Hartley and Zisserman, *Multiple view geometry in computer vision*. [≡](#) [▶](#)

# Matching points - why do we need a lot of them?



# RANSAC: fitting the data with gross outliers



<https://github.com/ducha-aiki/pyransac>

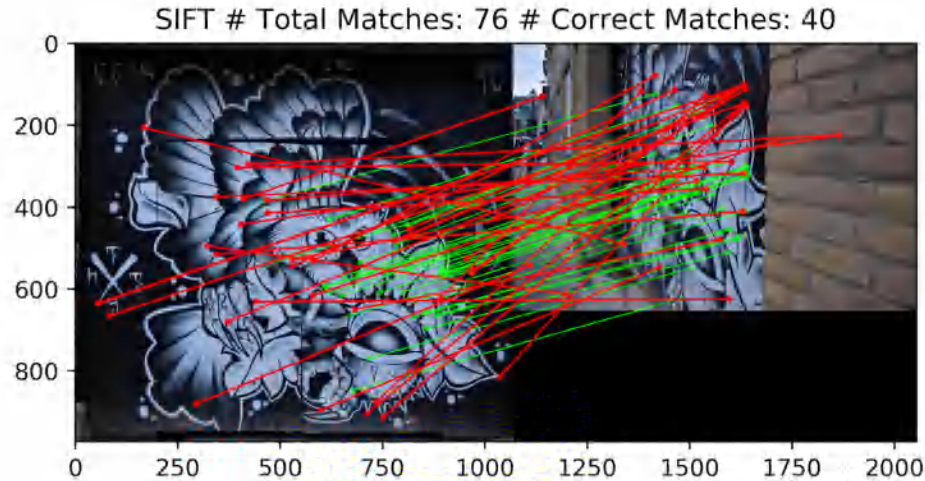


More details & info: Dmytro's talk  
at 10:00am

Image credit: <https://scipy-cookbook.readthedocs.io/items/RANSAC.html>



# Matching points - why do we need a lot of them?



# RANSAC: image matching example

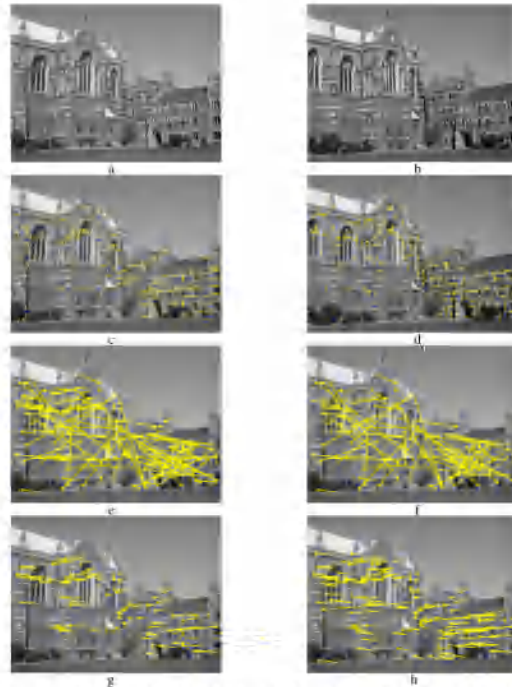


Fig. 11.4. Automatic computation of the fundamental matrix between two images using RANSAC. (a) (b) left and right images of Keble College, Oxford. The motion between views is a translation and rotation. The images are  $640 \times 480$  pixels. (c) (d) detected corners superimposed on the images. There are approximately 500 corners in each image. The following results are superimposed on the left image: (e) 188 putative matches shown by the line linking corners, note the clear mismatches; (f) outliers – 89 of the putative matches; (g) inliers – 99 correspondences consistent with the estimated F; (h) final set of 157 correspondences after guided matching and MLE. There are still a few mismatches evident, e.g. the lane line on the left.

# Recap

Better ways to match points between two images



Easier job for relative camera pose estimators



Better 3D models, panoramas, AR apps etc

# Classical pipeline



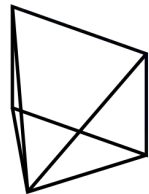
Scene B



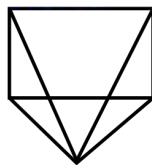
Scene A



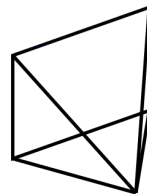
Scene C



*Camera Motion*<sub>A→B</sub>



*Camera Motion*<sub>A→C</sub>



# Classical pipeline

Detect



Describe



Match





# The classical image matching pipeline



- Step 1 *Detection*: Choose “interesting” points
- Step 2 *Description*: Convert the points to a suitable mathematical representation (descriptor)
- Step 3 *Matching*: Match the point descriptors between the two images



# Common types of feature frames



- ▶ Point:  $x, y$
- ▶ Circle:  $x, y, \rho$
- ▶ Rectangle:  $x, y, w, h$
- ▶ Oriented Circle:  $x, y, \rho, \theta$
- ▶ Ellipse:  $x, y, a, b$
- ▶ Oriented Ellipse:  $x, y, a, b, \theta$

# Feature frame/keypoint – Simplest Definition



$$f(x, y) = \sum_{(x_k, y_k) \in W} (I(x_k, y_k) - I(x_k + \Delta x, y_k + \Delta y))^2$$
$$f(x, y) \approx \sum_{(x, y) \in W} (I_x(x, y)\Delta x + I_y(x, y)\Delta y)^2$$

# Feature frame/keypoint – Simplest Definition



$$f(x, y) \approx (\Delta x \quad \Delta y) M \begin{pmatrix} \Delta x \\ \Delta y \end{pmatrix}$$

$$M = \begin{bmatrix} \sum_{(x,y) \in W} I_x^2 & \sum_{(x,y) \in W} I_x I_y \\ \sum_{(x,y) \in W} I_x I_y & \sum_{(x,y) \in W} I_y^2 \end{bmatrix}$$

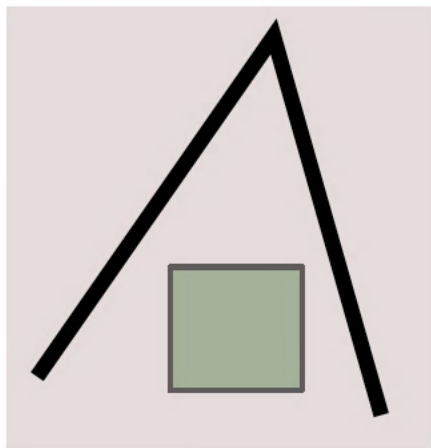
# Feature frame/keypoint – Simplest Definition

$$M = \begin{bmatrix} \sum_{(x,y) \in W} I_x^2 & \sum_{(x,y) \in W} I_x I_y \\ \sum_{(x,y) \in W} I_x I_y & \sum_{(x,y) \in W} I_y^2 \end{bmatrix}$$

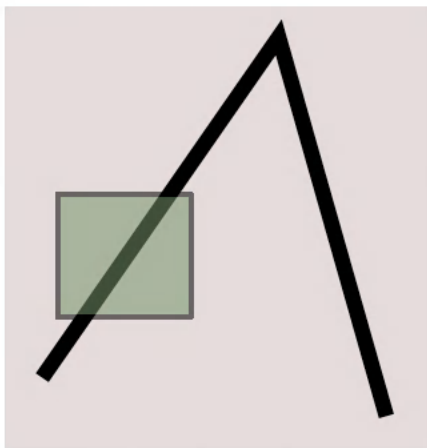
$\lambda_1, \lambda_2$ : Eigenvalues of  $M$

- ▶  $\lambda_1, \lambda_2 \approx 0$
- ▶  $\lambda_1 \gg \lambda_2$
- ▶  $\lambda_1 \ll \lambda_2$
- ▶  $\lambda_1 \approx \lambda_2 \gg 0$

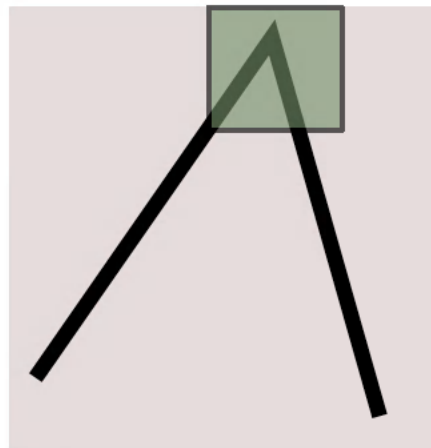
# Feature frame/keypoint – Simplest Definition



$$\lambda_1 \approx \lambda_2 \approx 0$$



$$\lambda_1 \gg \lambda_2$$

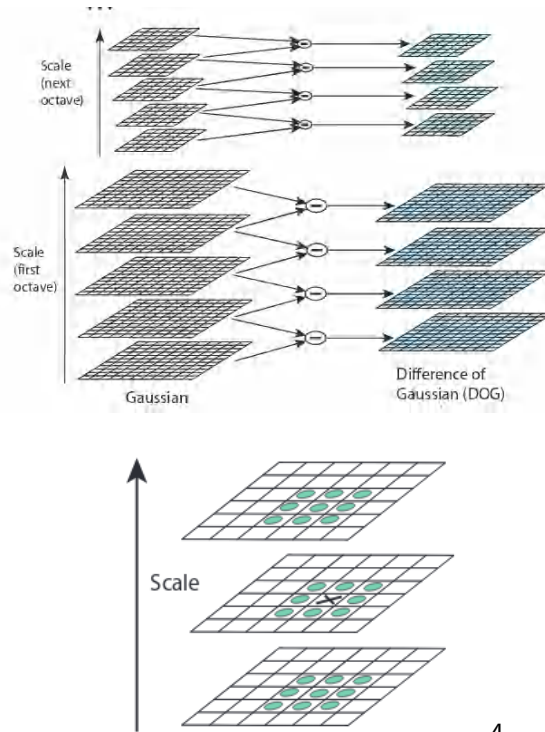


$$\lambda_1 \approx \lambda_2 \gg 0$$

# Adding scale estimation



# SIFT Detector



4

<sup>4</sup>Lowe, "Distinctive image features from scale-invariant keypoints".



# SURF

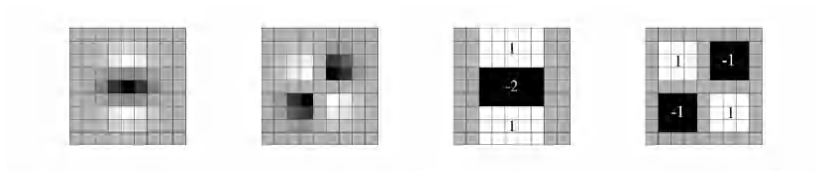


**Fig.1.** Left to right: the (discretised and cropped) Gaussian second order partial derivatives in  $y$ -direction and  $xy$ -direction, and our approximations thereof using box filters. The grey regions are equal to zero.

5

---

<sup>5</sup>Bay, Tuytelaars, and Van Gool, “Surf: Speeded up robust features”

## Edge Foci

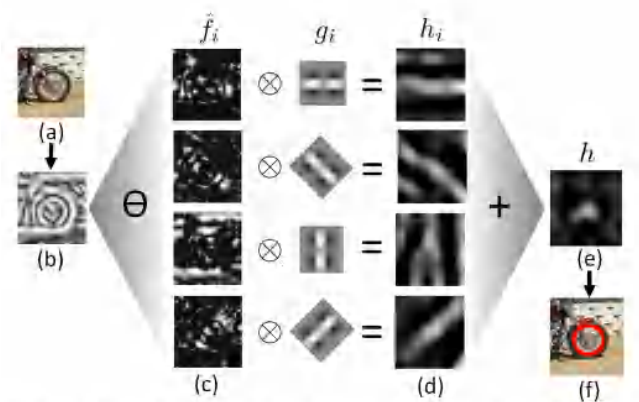
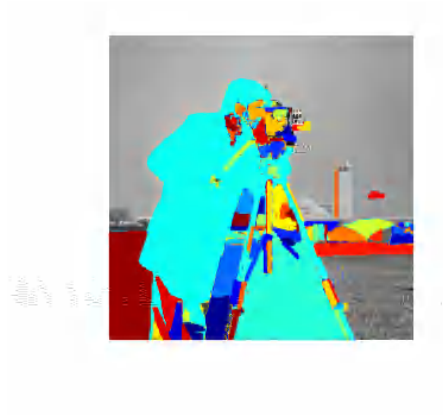


Figure 2. Flow diagram of the detector: (a) input image, (b) normalized gradient  $\hat{f}$ , (c) normalized gradients separated into orientations  $f_i$ , (d) responses after applying oriented filter  $h_i = \hat{f}_i \otimes g_i$ , (e) the aggregated results  $h$ , and (f) detected interest point.

7

# MSER

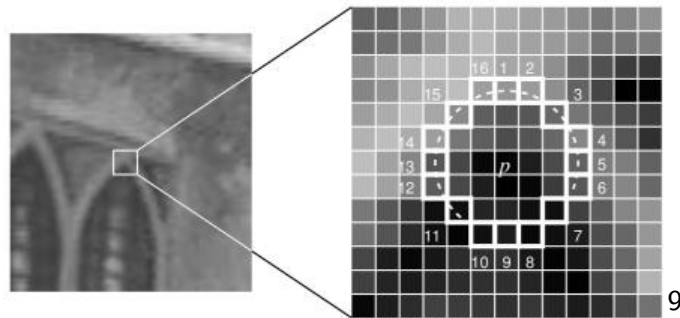


8

---

<sup>8</sup>Matas et al., “Robust wide-baseline stereo from maximally stable extremal regions”.

# FAST



---

<sup>9</sup>Rosten and Drummond, "Machine learning for high-speed corner detection".

- ▶ Many possibilities for types of feature frames
- ▶ Might include scale & orientation

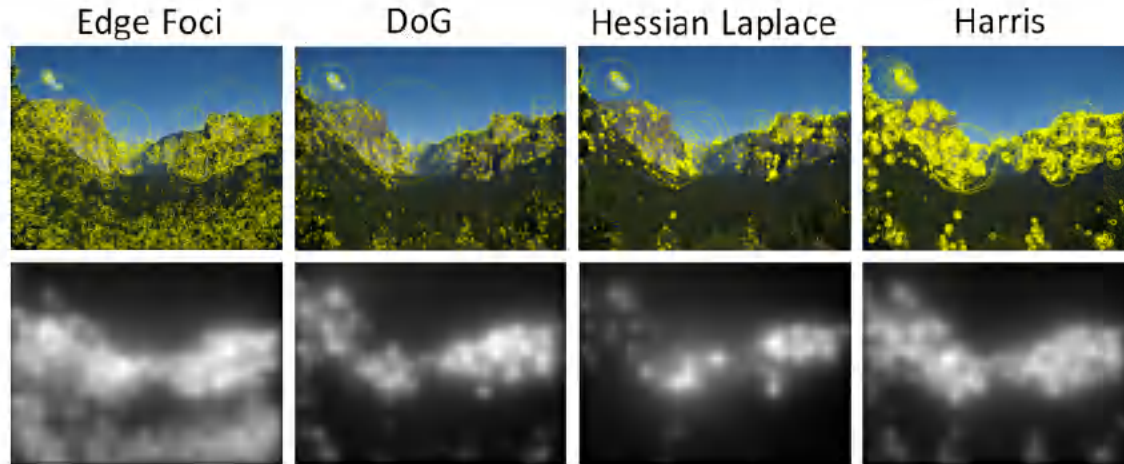


Figure 8. Visualization of the interest points and their spatial distributions for various detectors on Yosemite image.

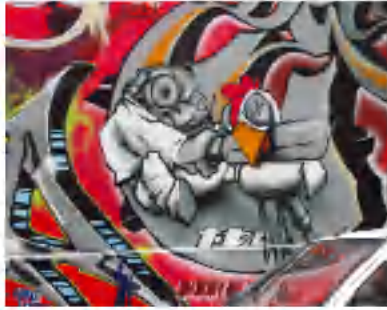
# From feature frames to patches



Detect Regions



Rectify patch around  
feature frame



Detect Regions

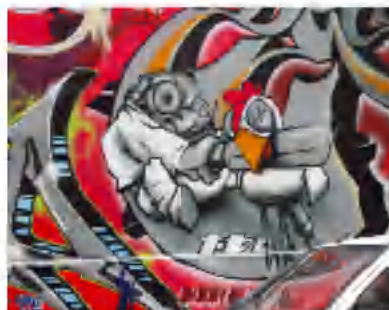


Rectify patch around  
feature frame

## Local Descriptor

A *vectorial representation* of the patch around a feature frame which is more a discriminative and robust than the patch.





Detect Regions



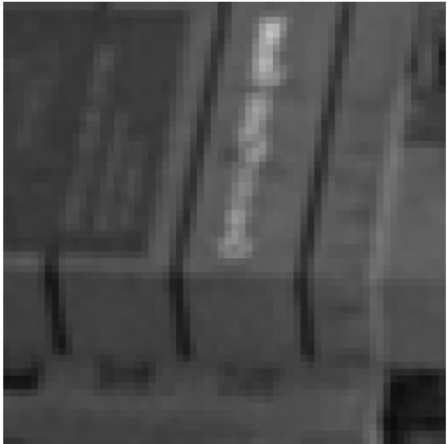
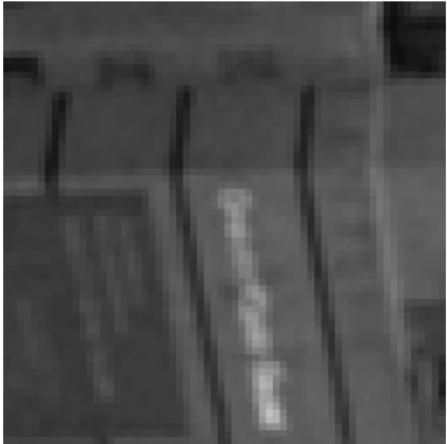
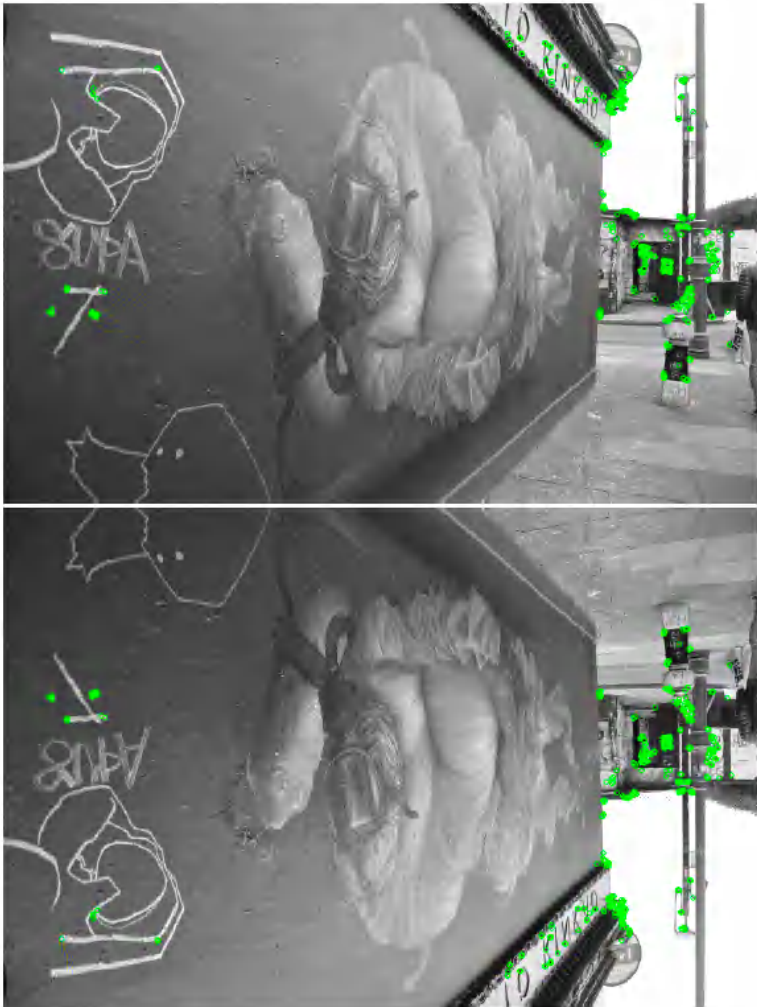
Rectify patch around  
feature frame

## Local Descriptor

A *vectorial representation* of the patch around a feature frame which is more a discriminative and robust than the patch.

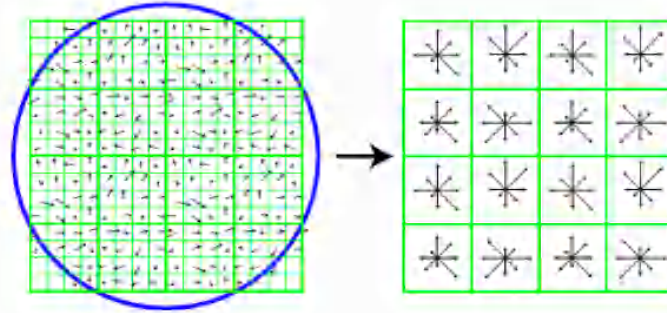


# Orientation



How to describe patches

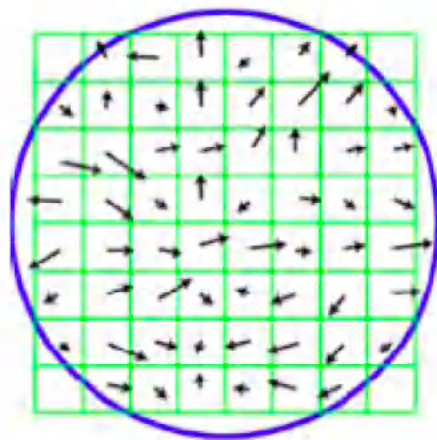
# SIFT



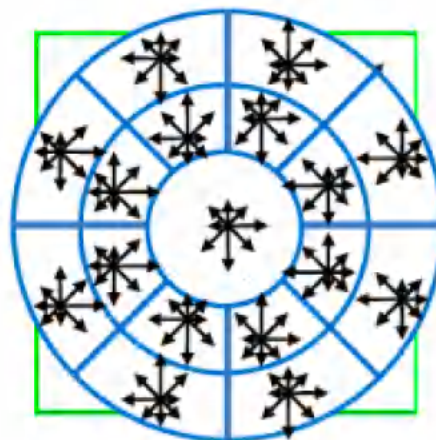
- ▶ The local spatial pooling of the descriptor is based on a rectangular grid that partitions the patch into several regions.
- ▶ Assuming the patch is divided into  $M$  rectangular areas, and the gradients are quantised to  $K$  angle bins, the resulting  $K$  dimensional histograms concatenated from  $M$  areas, will be represented by a point in the  $\mathbb{R}^{M \times K}$  space.
- ▶ In the case of the original implementation of SIFT, 16 grid quanta were combined with 8 angular bins, resulting in final dimensionality of 128.



# GLOH

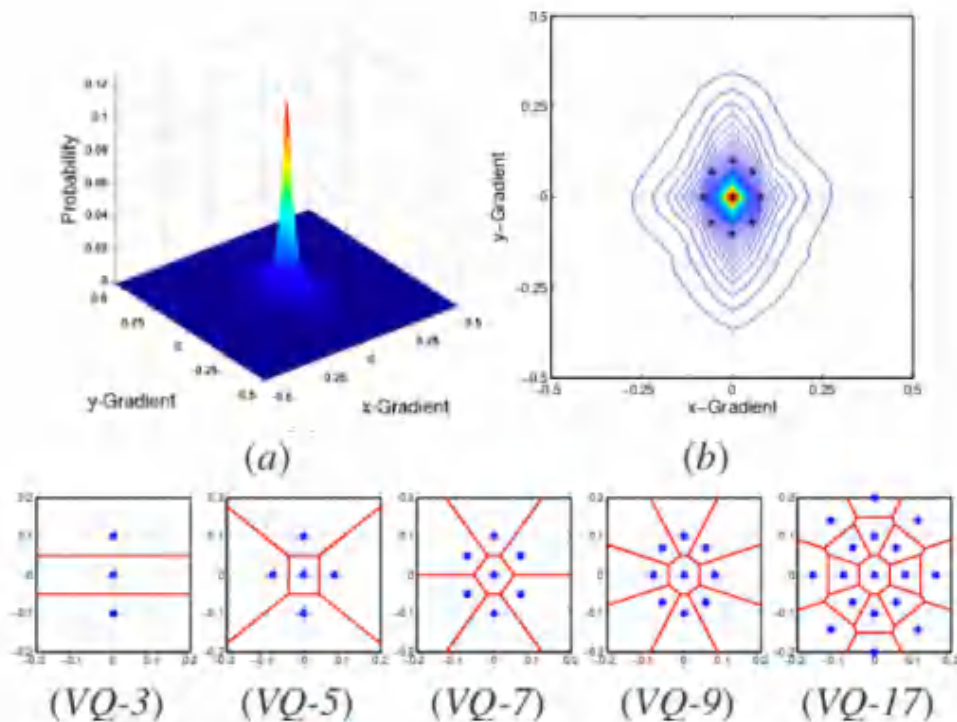


(a) image gradients



(b) keypoint descriptor

# CHoG





# DAISY

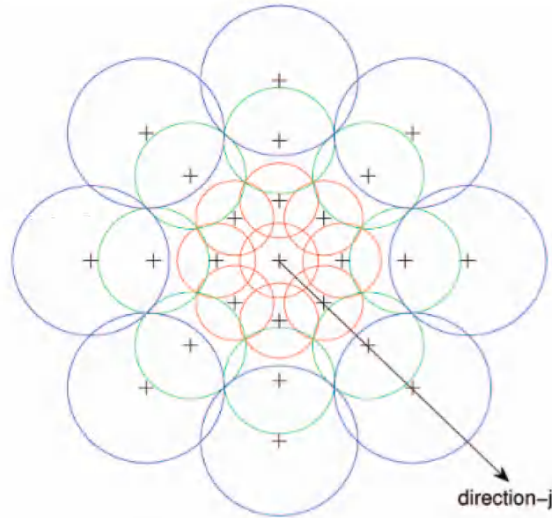
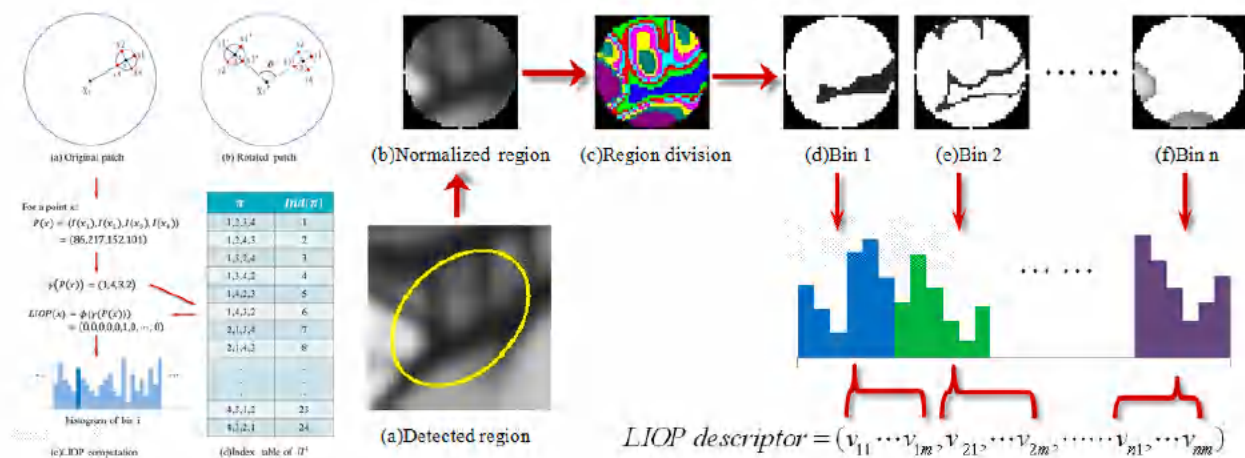


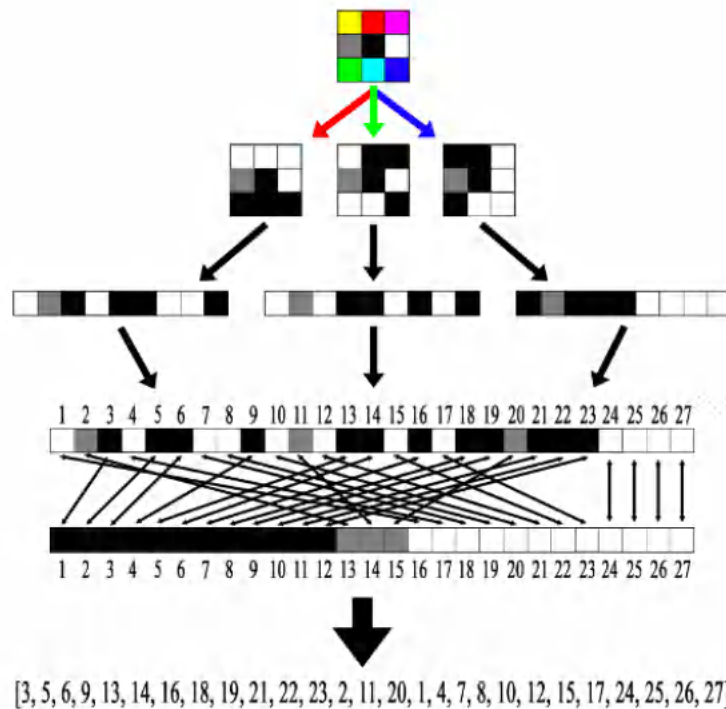
Fig. 6. The DAISY descriptor: Each circle represents a region where the radius is proportional to the standard deviations of the Gaussian kernels and the "+" sign represents the locations where we sample the convolved orientation maps center being a pixel location where we compute the descriptor. By overlapping the regions, we achieve smooth transitions between the regions and a degree of rotational robustness. The radii of the outer regions are increased to have an equal sampling of the rotational axis, which is necessary for robustness against rotation.

# LIOP



# LUCID

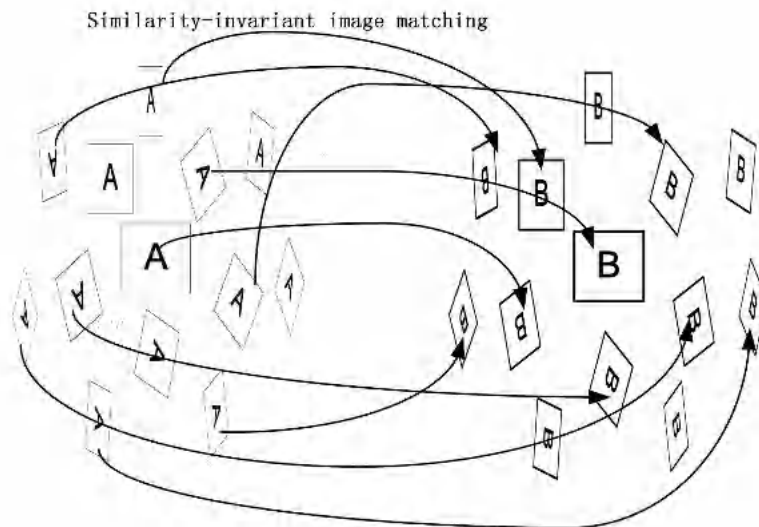
```
[~, desc1] = sort(p1(:));  
[~, desc2] = sort(p2(:));  
distance = sum(desc1 ~= desc2);
```



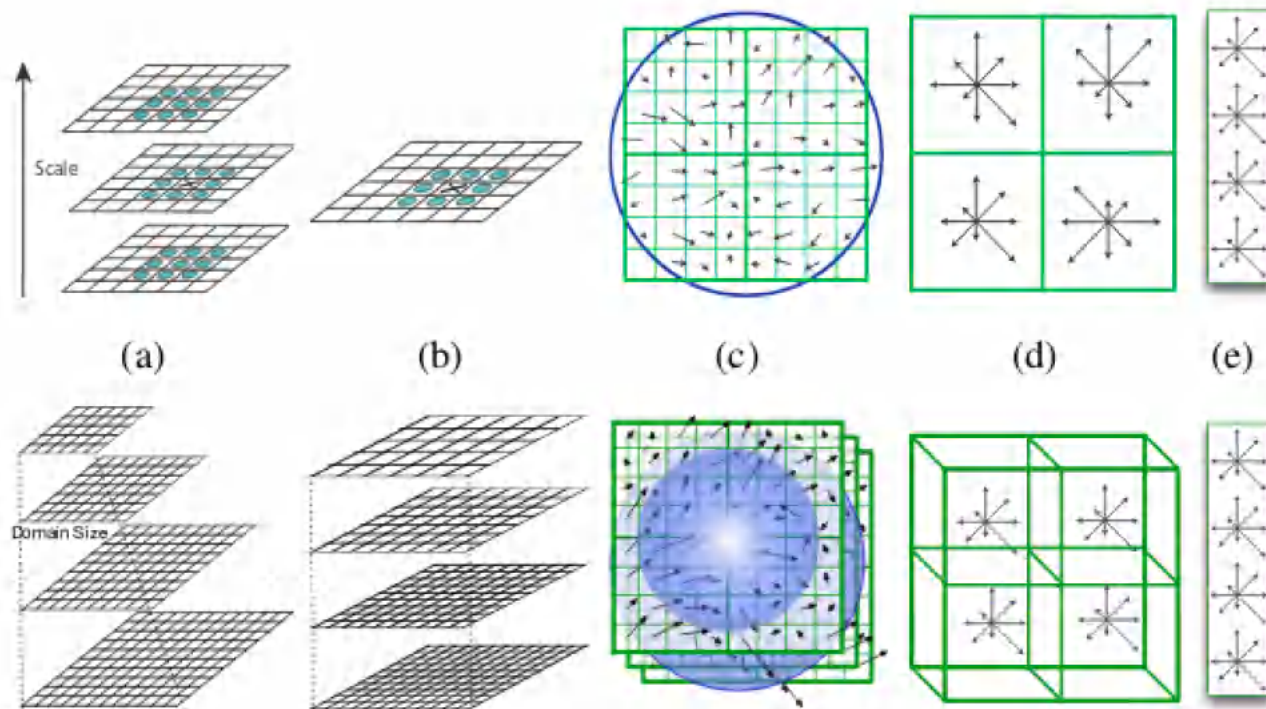
# Aggregation across scales and viewpoints

Several methods identified that aggregation across different scales or different viewpoints into a single feature vector can improve the discriminative power of the descriptor, albeit at the price of much higher computational cost.

# ASIFT



# DSP-SIFT



# Binary descriptors



# Hashing SIFT

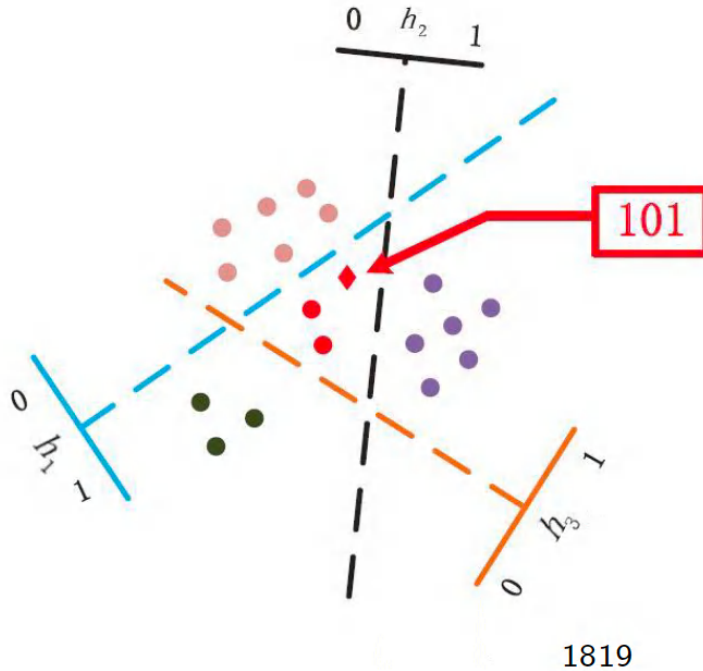
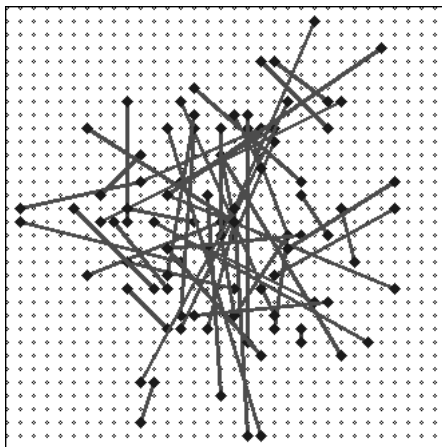


Image from Haisheng Li.

Terasawa and Tanaka, **Spherical LSH for approximate nearest neighbour search on unit hypersphere.**

Strecha et al., **LDAHash: Improved matching with [smaller descriptors](#).**

# BRIEF



# Learning-based descriptors

- From 2005 and on, more and more machine learning was utilised

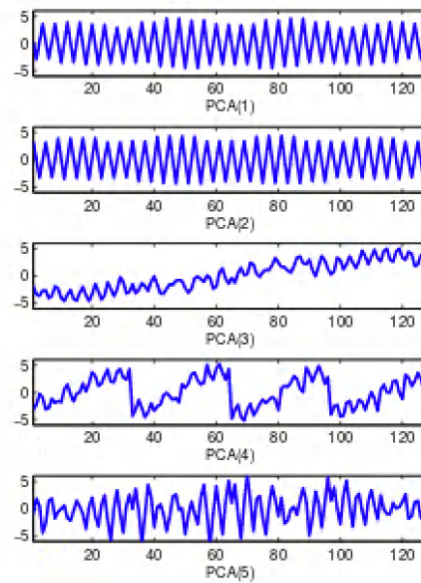
# PCA-SIFT

Collect a matrix  $X \in \mathbb{R}^{N \times D}$  with  $N$  descriptors of dimensionality  $D$

$$C = X^T X$$

$$C = U \Sigma V$$

Use the first  $K$  eigenvectors from  $U$  to project  $X$  to a new descriptor of size  $K$ .  $X_k = U_k X$ <sup>23</sup>



PCA



# Linear Projections

$$\begin{aligned}\mathbf{u}_{\text{LDP}} &= \arg \max_{\mathbf{u}} \frac{\sum_{(i,j) \in \mathcal{D}} \|\mathbf{u}^T \mathbf{x}_i - \mathbf{u}^T \mathbf{x}_j\|^2}{\sum_{(i,j) \in \mathcal{S}} \|\mathbf{u}^T \mathbf{x}_i - \mathbf{u}^T \mathbf{x}_j\|^2} \\ &= \arg \max_{\mathbf{u}} \frac{\mathbf{u}^T C_{\mathcal{D}} \mathbf{u}}{\mathbf{u}^T C_{\mathcal{S}} \mathbf{u}}\end{aligned}\quad (2)$$

Where  $C_{\mathcal{D}}$  and  $C_{\mathcal{S}}$  represent the inter- and intra-class covariance matrices of differently labeled points (unmatched features in image descriptor space) and same-labeled points (matched features), respectively.

$$C_{\mathcal{D}} \stackrel{\text{def}}{=} \sum_{(i,j) \in \mathcal{D}} (\mathbf{x}_i - \mathbf{x}_j)(\mathbf{x}_i - \mathbf{x}_j)^T \quad (3)$$

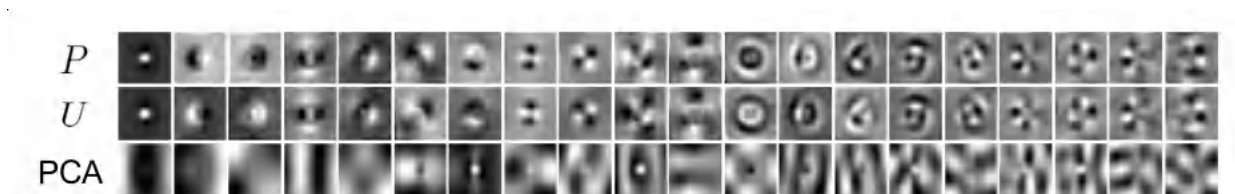
$$C_{\mathcal{S}} \stackrel{\text{def}}{=} \sum_{(i,j) \in \mathcal{S}} (\mathbf{x}_i - \mathbf{x}_j)(\mathbf{x}_i - \mathbf{x}_j)^T \quad (4)$$

Note that these are not the same matrices as the between-class  $S_B$  and within-class scatters  $S_W$  in equation (1) for LDA, although they are related (see section 3.3). The solution is the generalized eigenvectors:

$$U = \text{eig}(C_{\mathcal{S}}^{-1} C_{\mathcal{D}}) \quad (5)$$

The projection matrix is  $U \in \mathbb{R}^{m \times m'}$ , with  $m' \leq m$  eigenvectors corresponding to the  $m'$  largest eigenvalues.

# Linear Projections

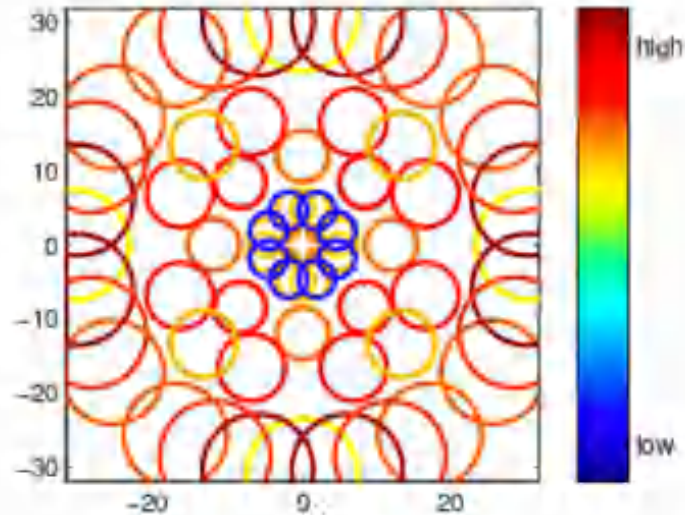




# Convex optimisation for learning descriptors

Learn optimal configuration of gaussian filters s.t.

$$\min_{\mathbf{y} \in P(\mathbf{x})} d_{\eta}(\mathbf{x}, \mathbf{y}) < \min_{\mathbf{u} \in N(\mathbf{x})} d_{\eta}(\mathbf{x}, \mathbf{u}),$$



# Deep Learning Era

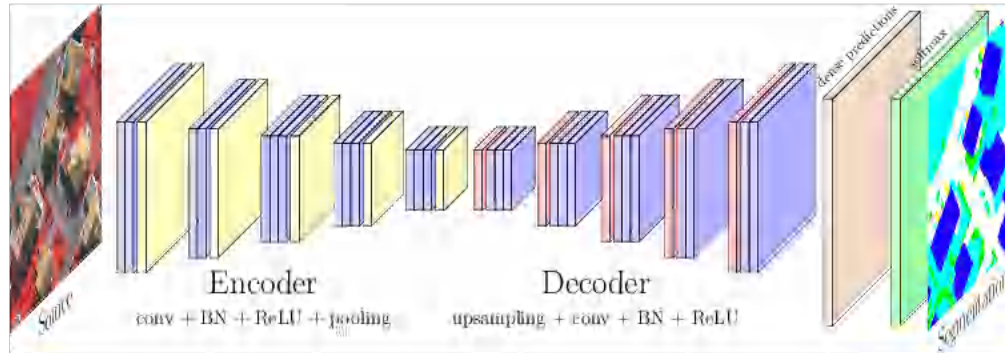
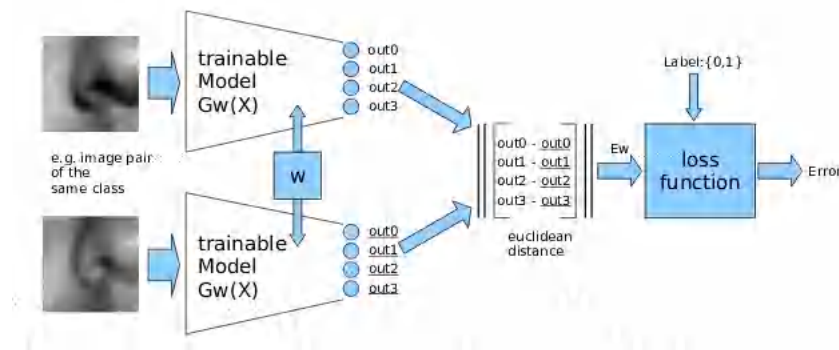


Image: Nicolas Audebert

# Early work (2008)

- Early work on learning convolutional neural networks as feature descriptors specifically for local patches, but was not immediately followed



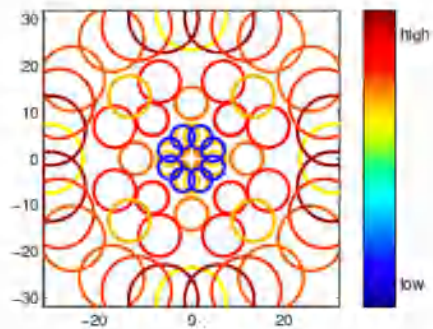
Jahrer, Grabner, and Bischof. **Learned local descriptors for recognition and matching.**

# Early work (2008)

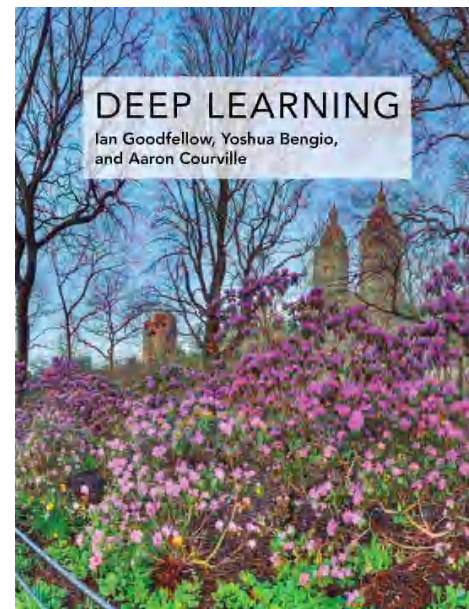


Learn optimal configuration of gaussian filters s.t.

$$\min_{\mathbf{y} \in P(\mathbf{x})} d_{\eta}(\mathbf{x}, \mathbf{y}) < \min_{\mathbf{u} \in N(\mathbf{x})} d_{\eta}(\mathbf{x}, \mathbf{u}),$$



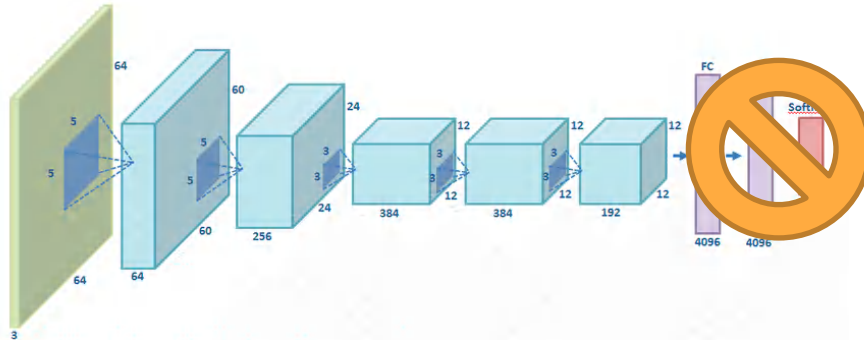
27



# The first “deep” success

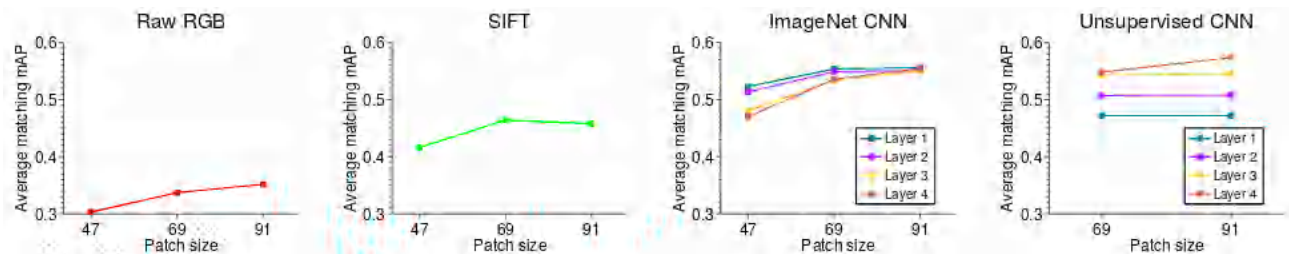


Get a network pre-trained on ImageNet



Remove FC layers & use features

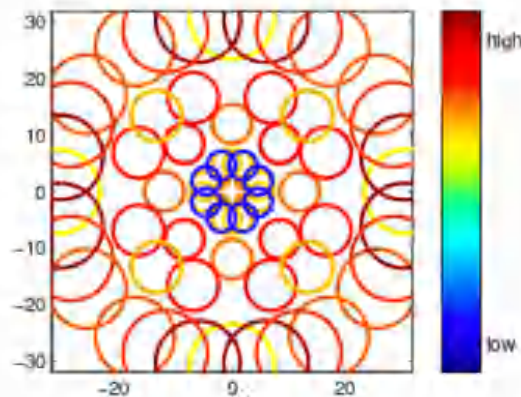
# The first “deep” success



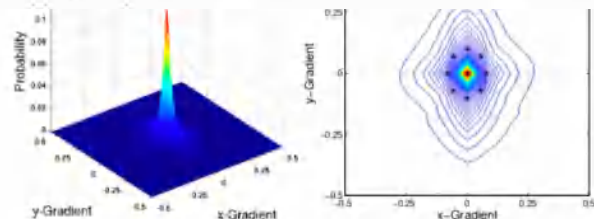


Learn optimal configuration of gaussian filters s.t.

$$\min_{y \in P(x)} d_{\eta}(x, y) < \min_{u \in N(x)} d_{\eta}(x, u),$$

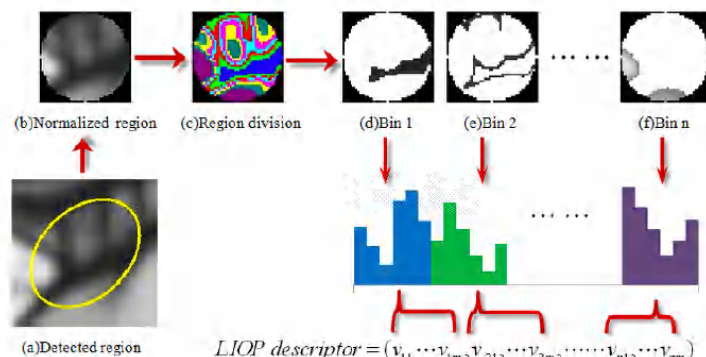
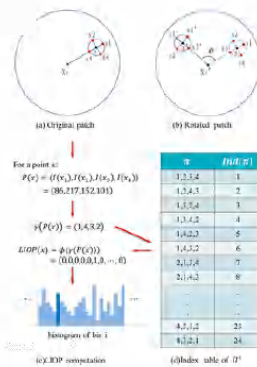
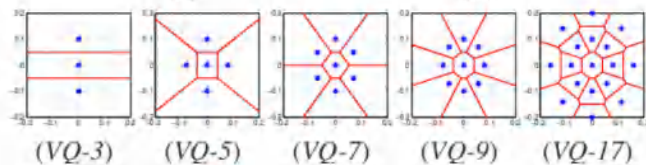


27



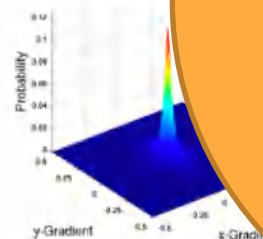
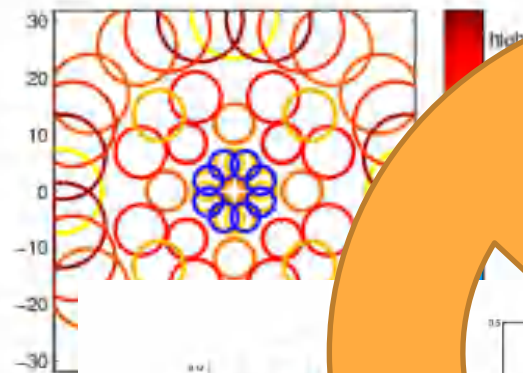
(a)

(b)

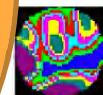
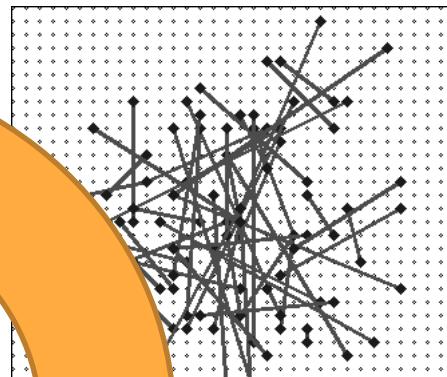
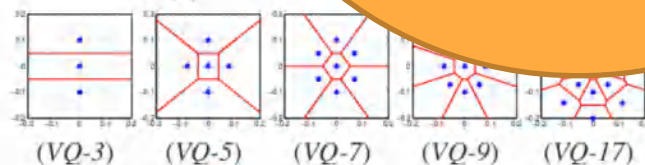


Learn optimal configuration of gaussian filters s.t.

$$\min_{y \in P(x)} d_{\eta}(x, y) < \min_{u \in N(x)} d_{\eta}(x, u),$$



(a)



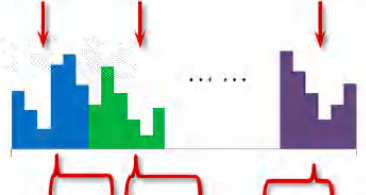
(c) Region division



(d) Bin 1

(e) Bin 2

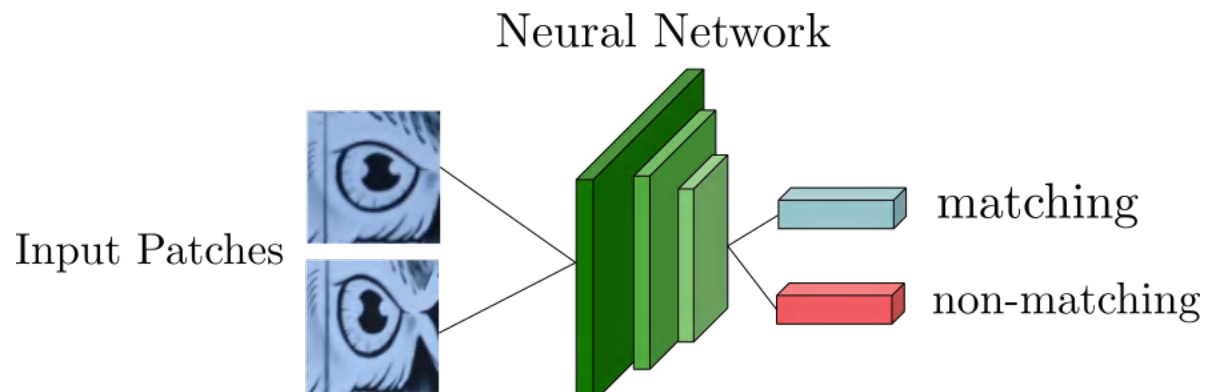
(f) Bin n



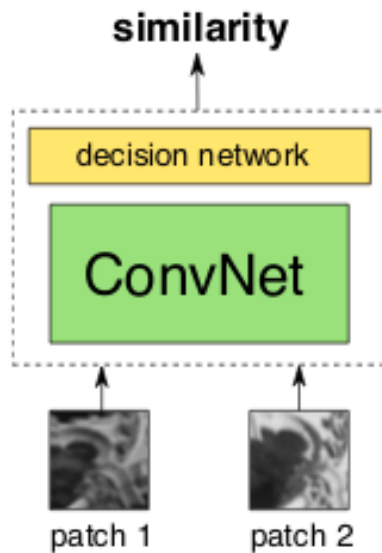
(a) Detected region

$$LIOP \text{ descriptor} = (v_{11}, \dots, v_{1m}, v_{21}, \dots, v_{2m}, \dots, v_{n1}, \dots, v_{nm})$$

# Deep learned descriptors



# DeepCompare



$$\min_w \frac{\lambda}{2} \|w\|_2 + \sum_{i=1}^N \max(0, 1 - y_i o_i^{net})$$

# DeepCompare

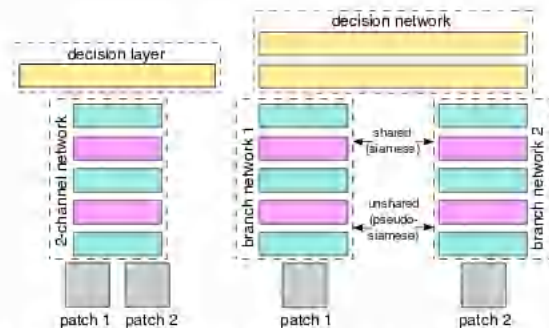


Figure 2. Three basic network architectures: 2-channel on the left, siamese and pseudo-siamese on the right (the difference between siamese and pseudo-siamese is that the latter does not have shared branches). Color code used: cyan = Conv+ReLU, purple = max pooling, yellow = fully connected layer (ReLU exists between fully connected layers as well).

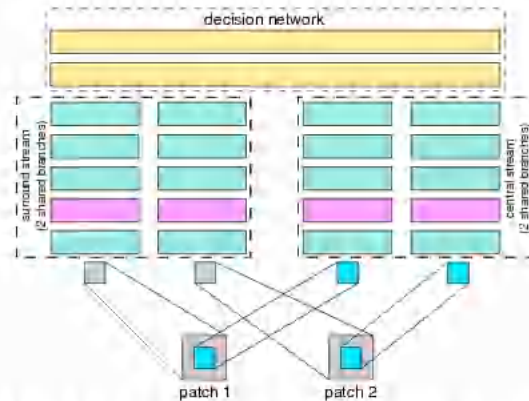
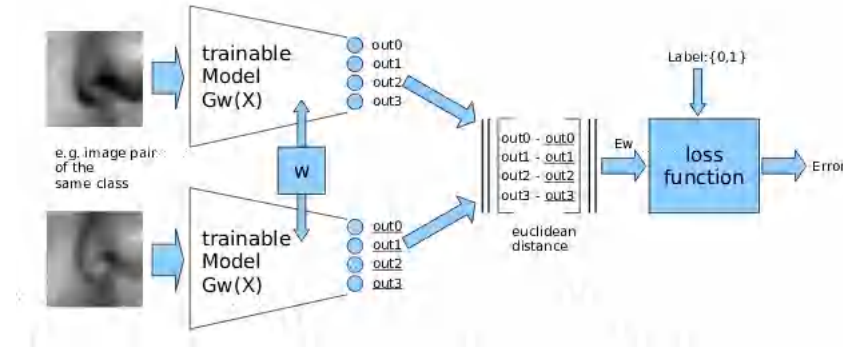


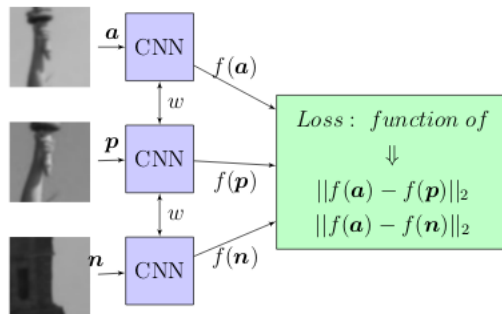
Figure 3. A central-surround two-stream network that uses a siamese-type architecture to process each stream. This results in 4 branches in total that are given as input to the top decision layer (the two branches in each stream are shared in this case).

# Reminder: Early work (2008)



Jahrer, Grabner, and Bischof. **Learned local descriptors for recognition and matching.**

# TFeat

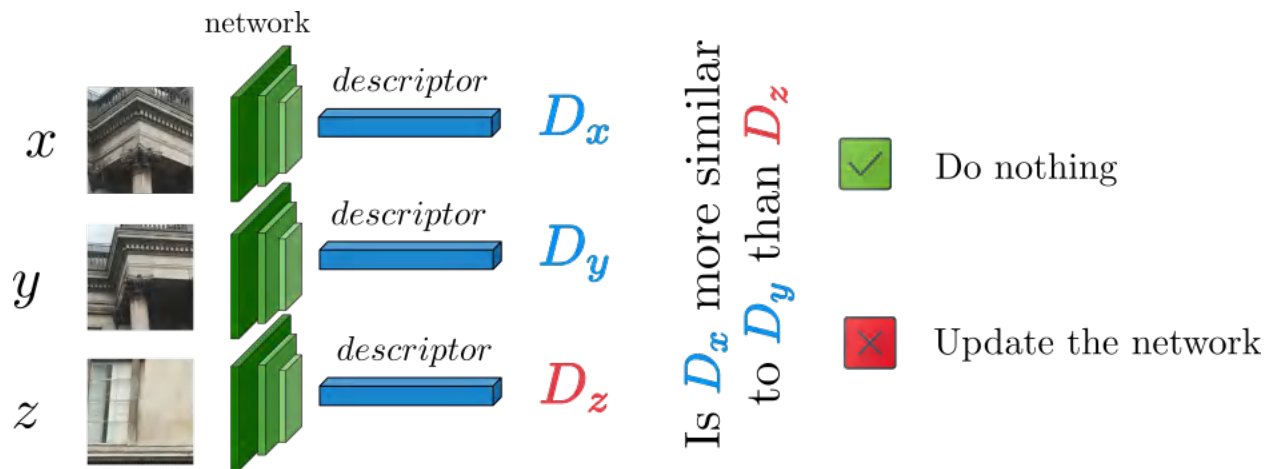


$$\sum_{i=1}^N l_{rank}(\delta_+, \delta_-) + \lambda \cdot \|w\|_2^2$$

where

$$l_{rank}(\delta_+, \delta_-) = \max(0, \mu + \delta_+ - \delta_-)$$

# Triplet Learning





# L2-Net



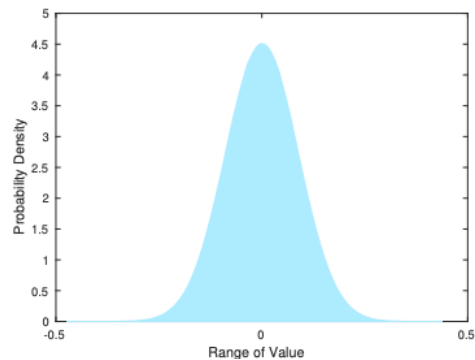
- $E_1$ : Similarity loss
- $E_2$ : Compactness loss
- $E_3$ : Intermediate feature maps loss

$$E_1 = -\frac{1}{2} \left( \sum_i \log s_{ii}^c + \sum_i \log s_{ii}^r \right)$$

$$E_2 = \frac{1}{2} \left( \sum_{i \neq j} (r_{ij}^1)^2 + \sum_{i \neq j} (r_{ij}^2)^2 \right)$$

$$E_3 = -\frac{1}{2} \left( \sum_i \log v_{ii}^c + \sum_i \log v_{ii}^r \right)$$

# Binary L2-Net

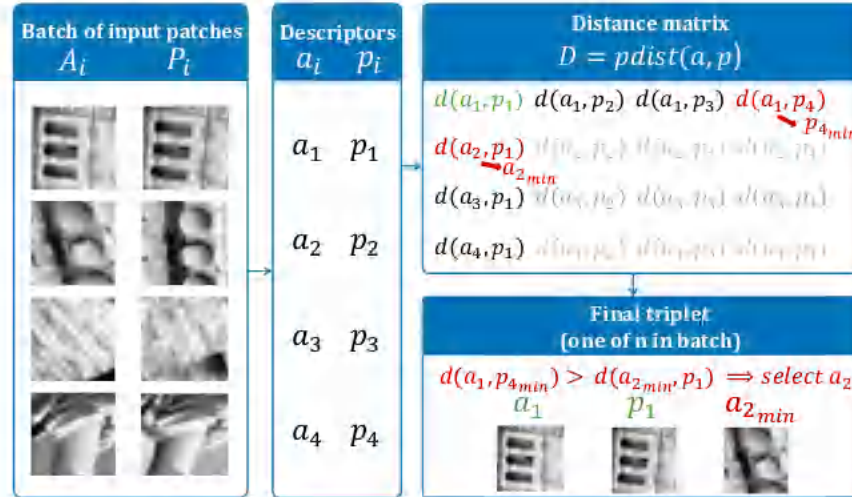


use sign of output

Test	Liberty	Notredame	Yosemite	Mean
L2-Net	4.16	1.54	4.41	3.37
L2-Net+	3.2	1.3	3.6	2.7
CS L2-Net	2.43	0.92	2.58	1.97
CS L2-Net+	<b>1.9</b>	<b>0.73</b>	<b>1.85</b>	<b>1.49</b>
Binary L2-Net	12.4	6.4	13.16	10.65
Binary L2-Net+	10.74	5.44	11.07	9.08
Binary CS L2-Net	6.43	2.88	6.91	5.4
Binary CS L2-Net+	<b>5.4</b>	<b>2.44</b>	<b>5.88</b>	<b>4.57</b>

Table 2. Performance of networks on the Brown dataset when they are trained on HPatches dataset .

# HardNet



# HardNet

Table 1: Patch correspondence verification performance on the Brown dataset. We report false positive rate at true positive rate equal to 95% (FPR95). **Some papers report false discovery rate (FDR) instead of FPR due to bug in the source code.** For consistency we provide FPR, either obtained from the original article or re-estimated from the given FDR (marked with \*). The best results are in **bold**.

Training	Notredame	Yosemite	Liberty	Yosemite	Liberty	Notredame	Mean	
Test	Liberty		Notredame		Yosemite		FDR	FPR
SIFT [9]	29.84		22.53		27.29			26.55
MitchNet* [14]	7.04	11.47	3.82	5.65	11.6	8.7	7.74	8.05
TFeat-M* [23]	7.39	10.31	3.06	3.8	8.06	7.24	6.47	6.64
PCW [33]	7.44	9.84	3.48	3.54	6.56	5.02		5.98
L2Net [24]	3.64	5.29	1.15	1.62	4.43	3.30		3.24
HardNetNIPS	3.06	3.27	0.96	1.4	3.04	2.53	3.00	2.54
HardNet	<b>1.47</b>	<b>2.67</b>	<b>0.62</b>	<b>0.88</b>	<b>2.14</b>	<b>1.65</b>		<b>1.57</b>
Augmentation: flip, 90° random rotation								
GLoss+ [31]	3.69	4.91	0.77	1.14	3.09	2.67		3.71
DC2ch2st+ [15]	4.55	7.2	1.9	2.11	5.00	4.10		4.19
L2Net+ [24] +	2.36	4.7	0.72	1.29	2.57	<b>1.71</b>		2.23
HardNet+NIPS	2.28	3.25	0.57	0.96	2.13	2.22	1.97	1.9
HardNet+	<b>1.49</b>	<b>2.51</b>	<b>0.53</b>	<b>0.78</b>	<b>1.96</b>	1.84		<b>1.51</b>

# SOSNet

## First Order Similarity Loss

$$\mathcal{L}_{\text{FOS}} = \frac{1}{N} \sum_{i=1}^N \max(0, t + d_i^{\text{pos}} - d_i^{\text{neg}})^2,$$
$$d_i^{\text{pos}} = d(\mathbf{x}_i, \mathbf{x}_i^+),$$
$$d_i^{\text{neg}} = \min_{\forall j, j \neq i} (d(\mathbf{x}_i, \mathbf{x}_j), d(\mathbf{x}_i, \mathbf{x}_j^+), d(\mathbf{x}_i^+, \mathbf{x}_j), d(\mathbf{x}_i^+, \mathbf{x}_j^+)),$$

## Second Order Similarity Loss

$$d^{(2)}(\mathbf{x}_i, \mathbf{x}_i^+) = \sqrt{\sum_{j \neq i}^N (d(\mathbf{x}_i, \mathbf{x}_j) - d(\mathbf{x}_i^+, \mathbf{x}_j^+))^2},$$

$$\mathcal{R}_{\text{SOS}} = \frac{1}{N} \sum_{i=1}^N d^{(2)}(\mathbf{x}_i, \mathbf{x}_i^+).$$

$$\mathcal{L}_{\text{T}} = \mathcal{L}_{\text{FOS}} + \mathcal{R}_{\text{SOS}},$$

**SOSNet: Second Order Similarity Regularization for Local Descriptor Learning**

Yurun Tian, Xin Yu, Bin Fan, Fuchao Wu, Huub Heijnen, Vassileios Balntas

# SOSNet

Second order consistency between classes

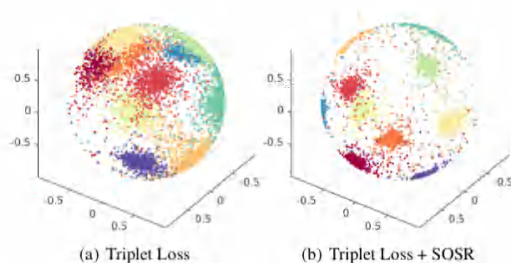
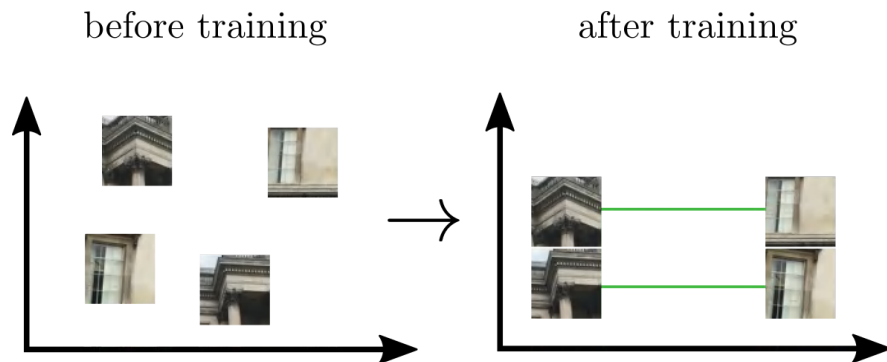


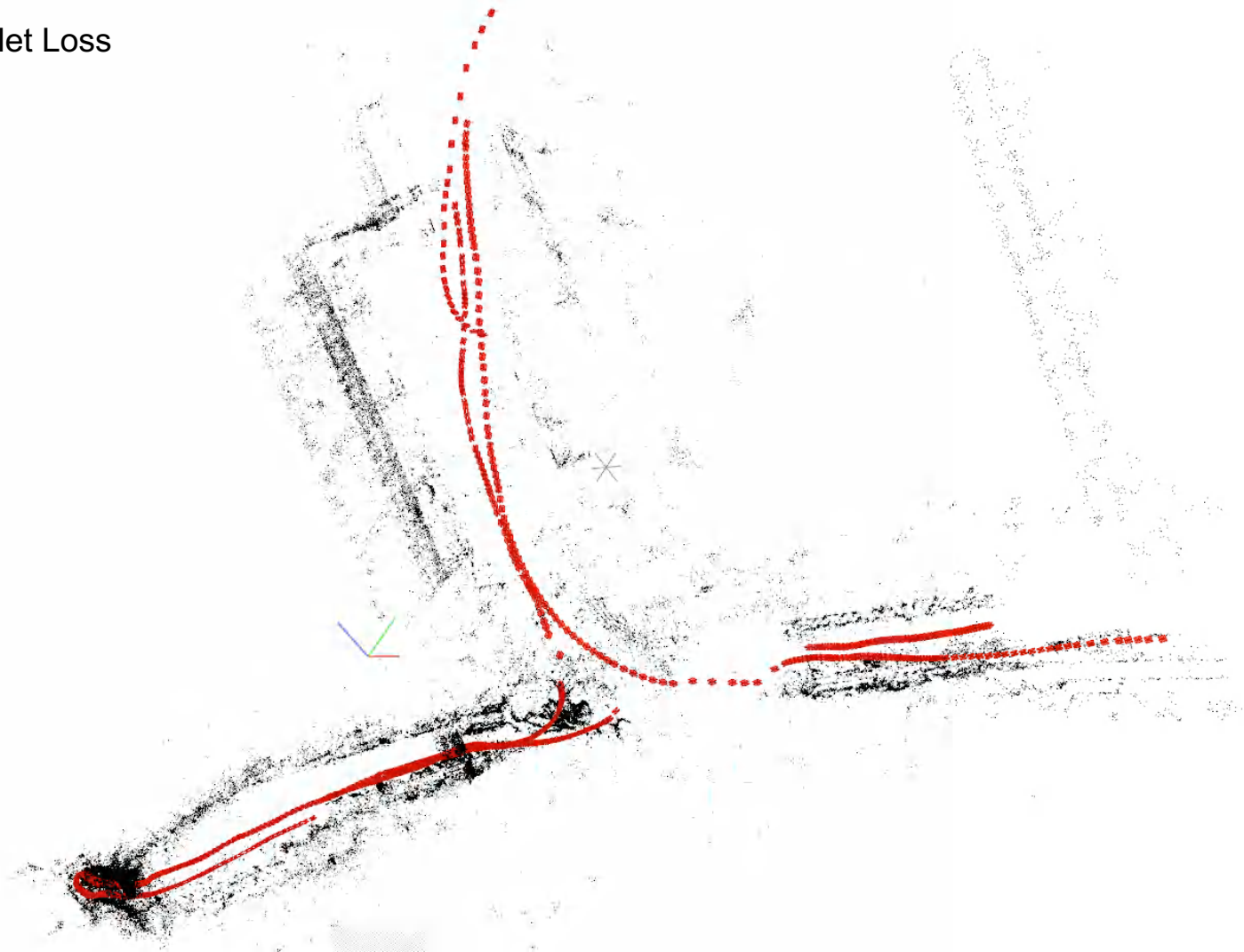
Figure 1. Qualitative results of our proposed SOSR on features learned for the 10 digits of the MNIST [19] dataset. Each digit is represented by a different colour on the unit sphere. We can observe that by using our SOSR method that encourages second order similarity, more compact individual clusters are learned compared to standard triplet loss.



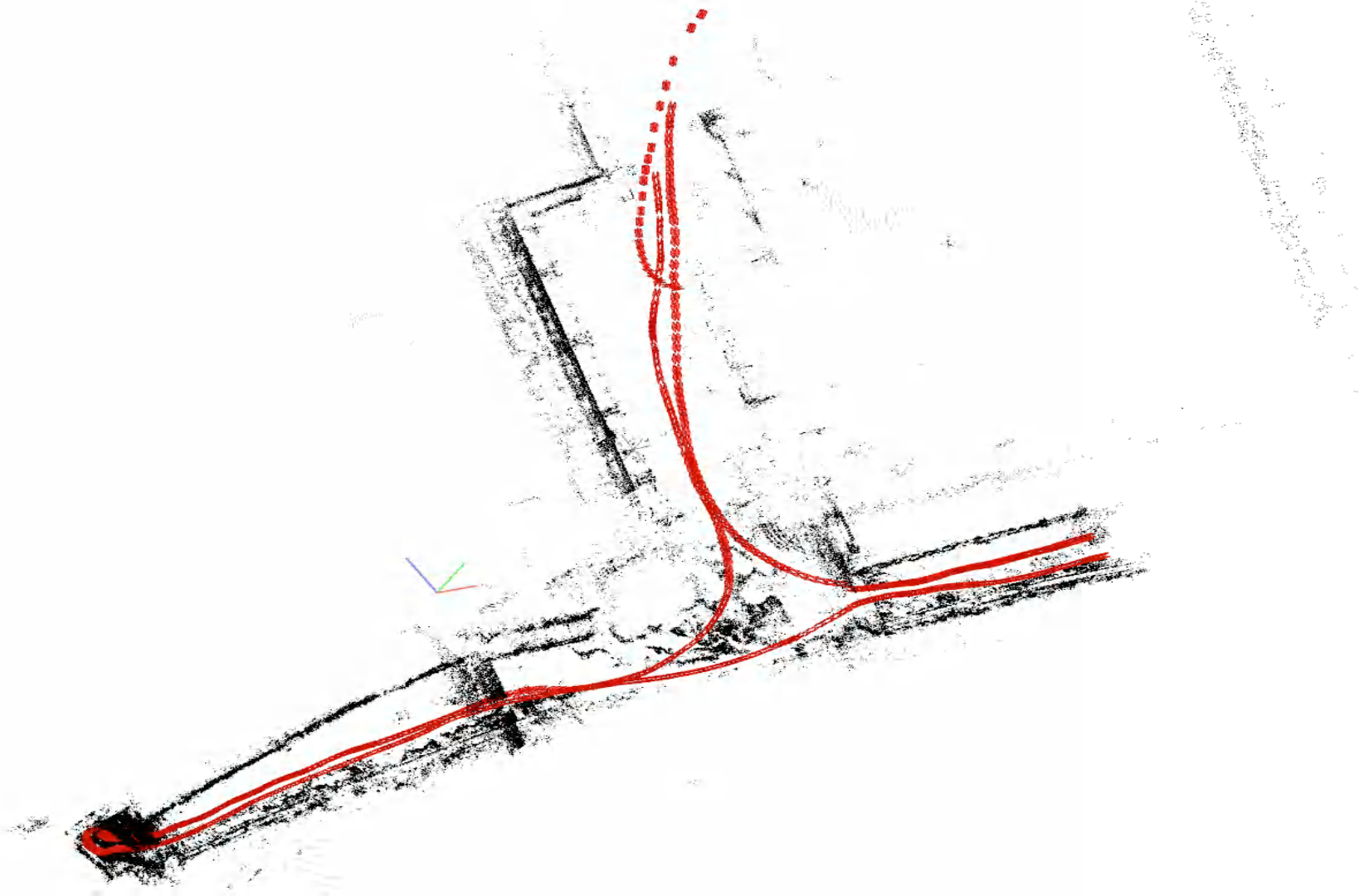
**SOSNet: Second Order Similarity Regularization for Local Descriptor Learning**

Yurun Tian, Xin Yu, Bin Fan, Fuchao Wu, Huub Heijnen, Vassileios Balntas

Triplet Loss



SOS





# Current status: classical pipeline

SOSNet # Total Matches: 263 # Correct Matches: 262



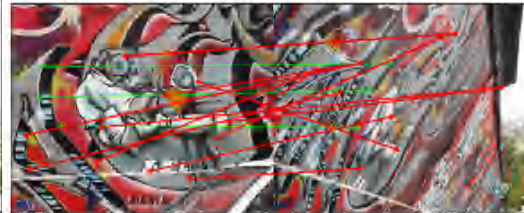
SIFT # Total Matches: 186 # Correct Matches: 163



SOSNet # Total Matches: 12 # Correct Matches: 10



SIFT # Total Matches: 18 # Correct Matches: 3



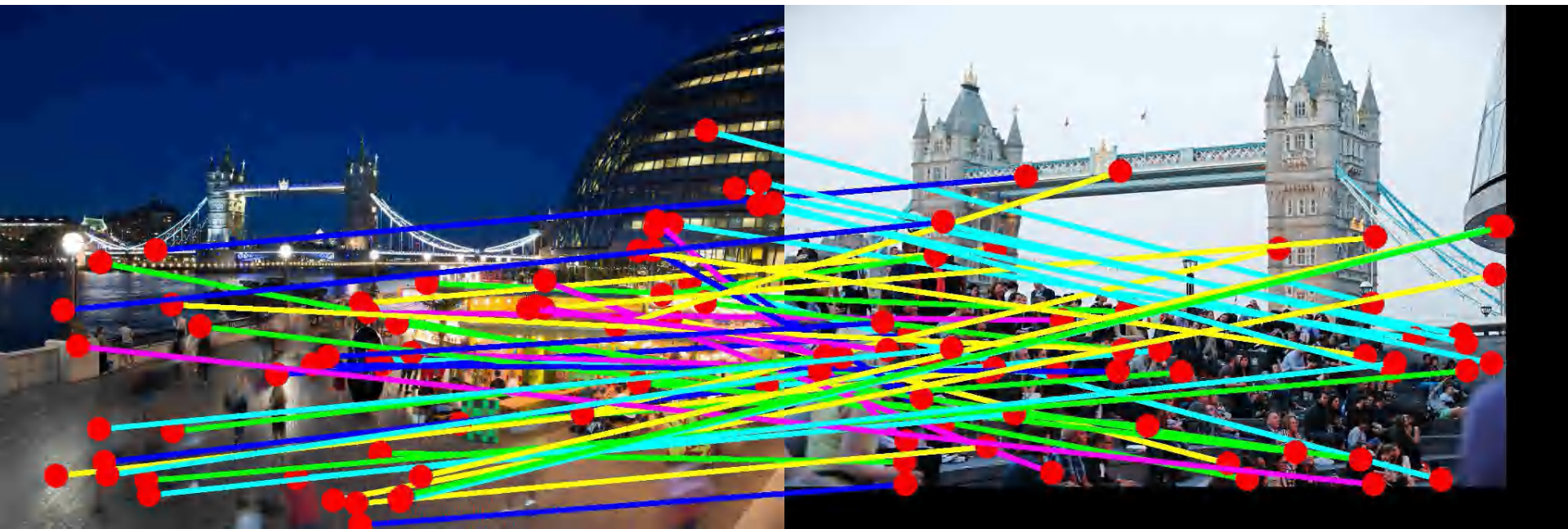
SOSNet # Total Matches: 120 # Correct Matches: 120



SIFT # Total Matches: 76 # Correct Matches: 40



# Limits of the “classical pipeline”



# Classical pipeline

Detect



Describe



Match



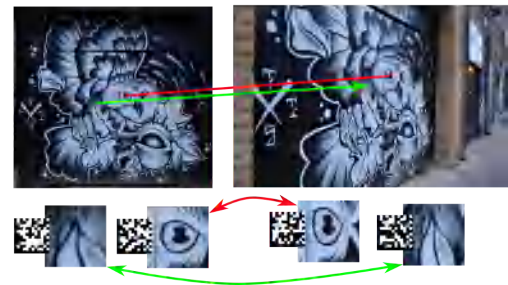
# Classical pipeline replacement?

Detect



Describe

Match





# Classical pipeline replacement?

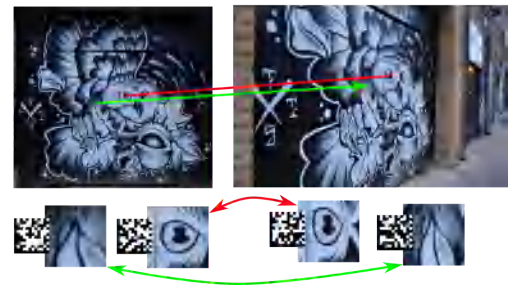
Detect



Describe



Match



\*Maybe some parts only

# Limits of the “classical pipeline”

- New methods are needed that are based on modern networks, including end to end training of networks
- Need to abstract more than the “keypoint” & “patch” paradigms.



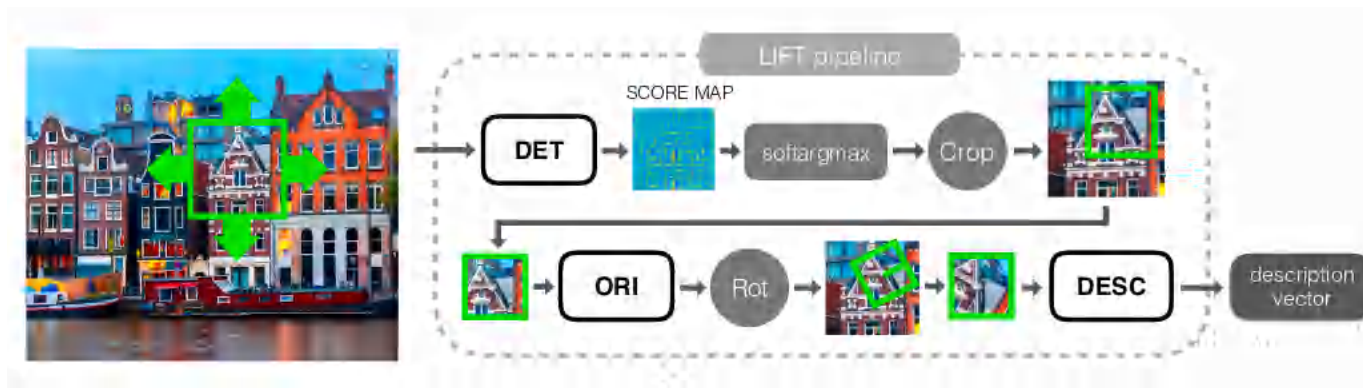
## “Modern” Methods

# Modern methods

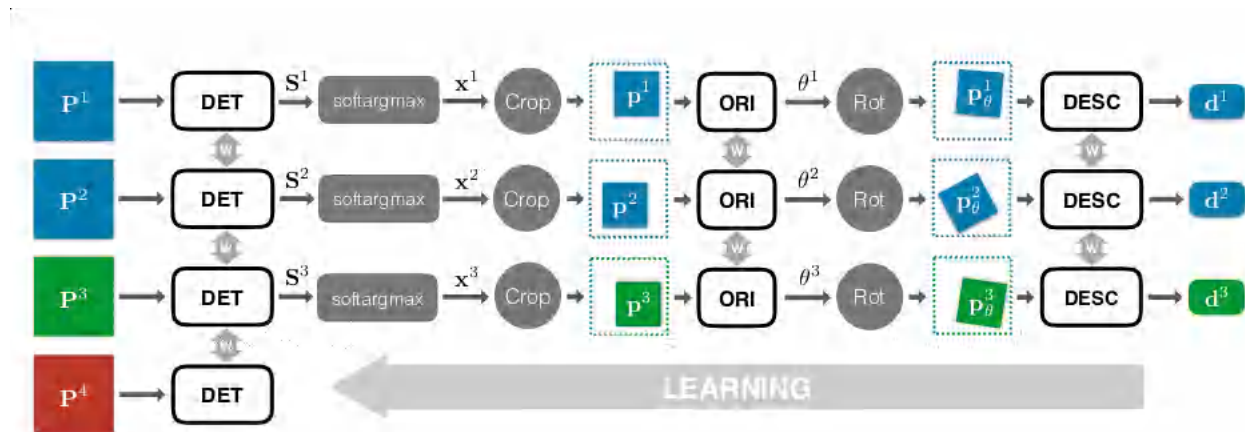
- Replace some/all parts of the classical pipeline
- Focus on training as much as possible end-to-end
- Focus on new matching methods, other than *argmins* of distance matrix



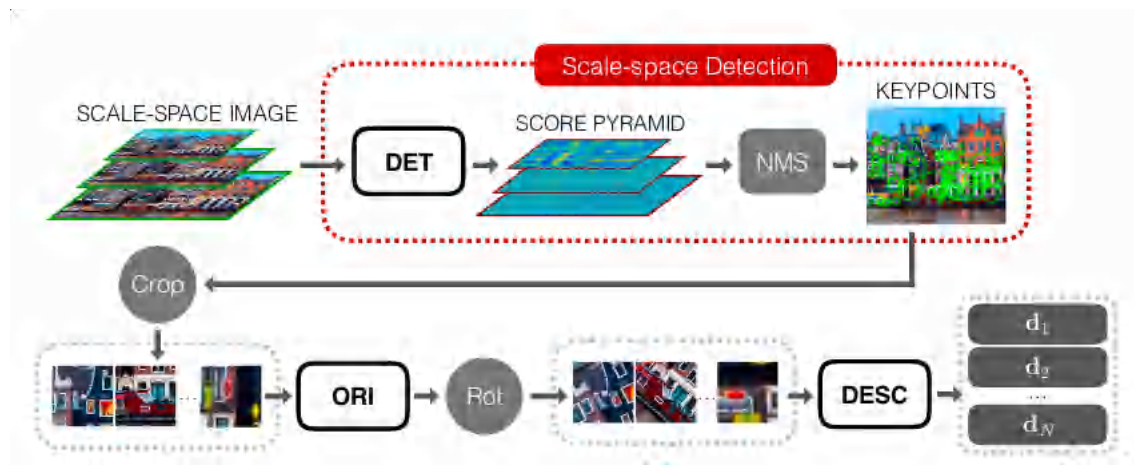
# LIFT



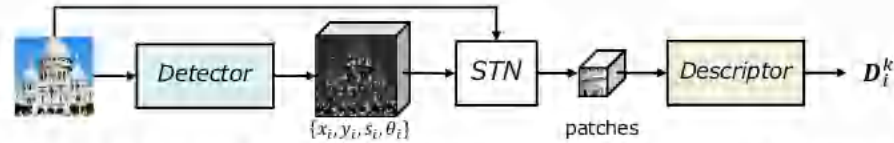
# LIFT



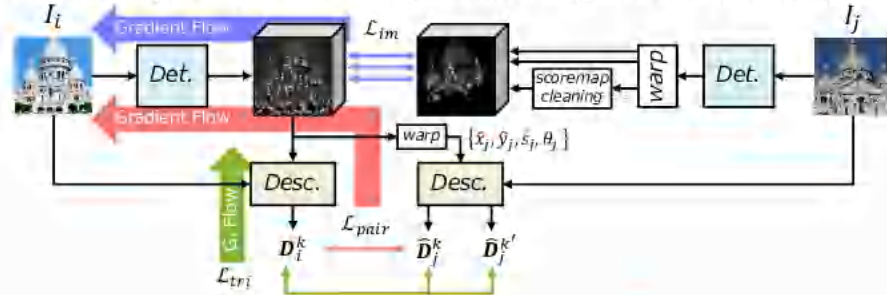
# LIFT



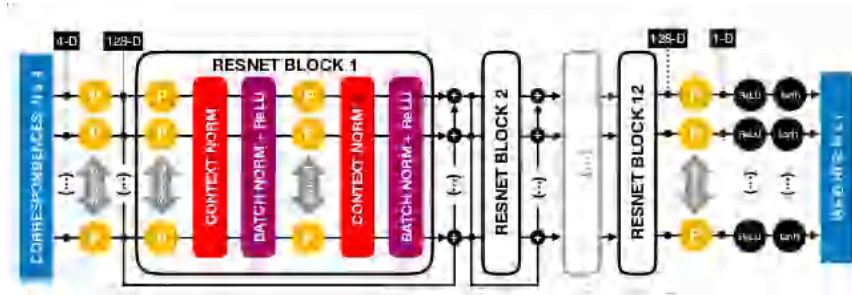
# LF-Net



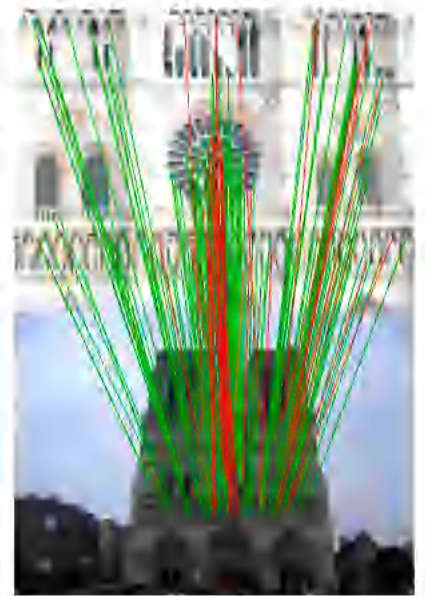
(a) The LF-Net architecture. The *detector* network generates a scale-space score map along with dense orientation estimates, which are used to select the keypoints. Image patches around the chosen keypoints are cropped with a differentiable sampler (STN) and fed to the *descriptor* network, which generates a descriptor for each patch.



# Learning correspondences



(a) RANSAC



(b) Our approach

# Superpoint

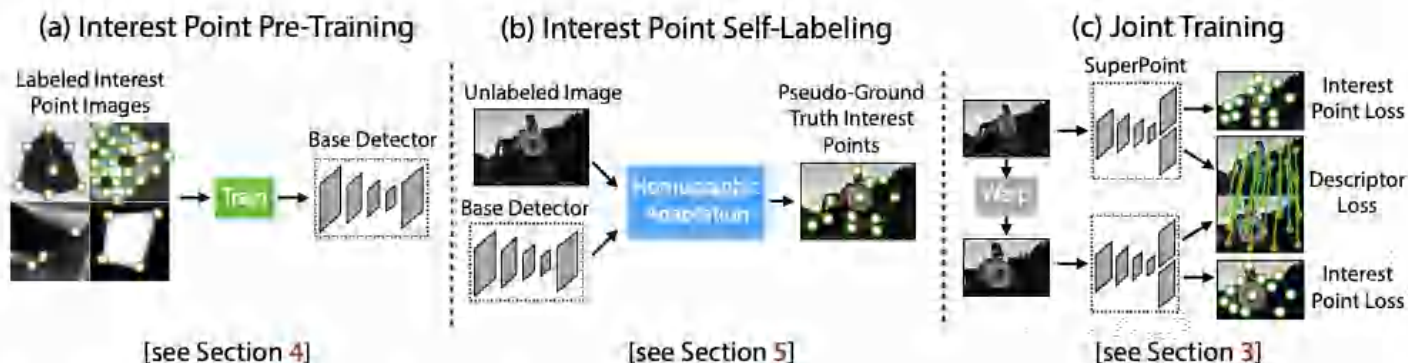
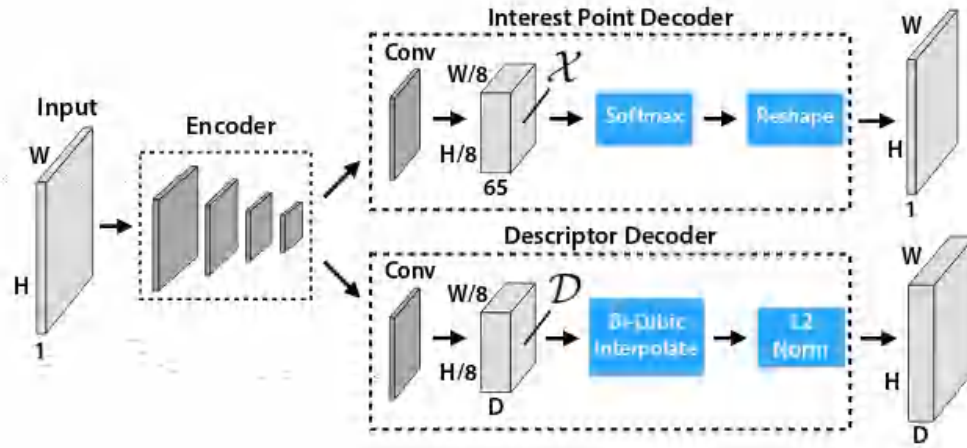


Figure 2. **Self-Supervised Training Overview.** In our self-supervised approach, we (a) pre-train an initial interest point detector on synthetic data and (b) apply a novel Homographic Adaptation procedure to automatically label images from a target, unlabeled domain. The generated labels are used to (c) train a fully-convolutional network that jointly extracts interest points and descriptors from an image.

# Superpoint



DeTone, Malisiewicz, and Rabinovich, SuperPoint: Self-Supervised Interest Point Detection and Description



# Implicitly Matched Interest Points (IMIPs)

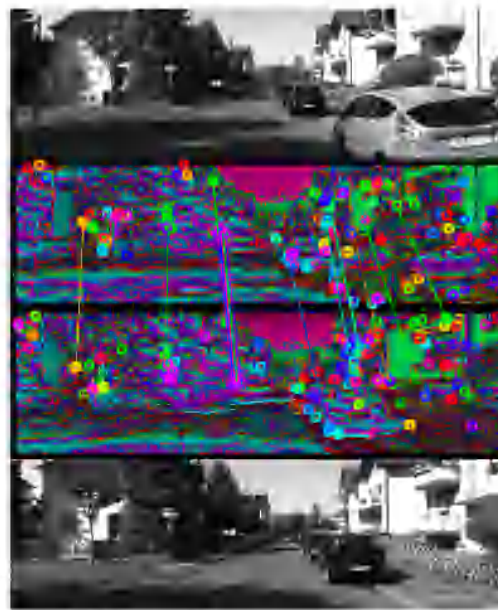


Figure 1. We propose a CNN interest point detector which provides implicitly matched interest points — descriptors are not needed for matching. This image illustrates the output of the final layer, which determines the interest points. Hue indicates which channel has the strongest response for a given pixel, and brightness indicates that response. Circles indicate the 128 interest points, which are the global maxima of each channel. Circle thicknesses indicate confidence in a point. Lines indicate inferior matches after P3P localization.



# DELF

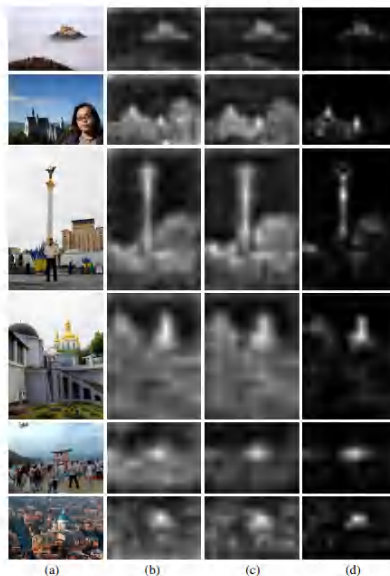
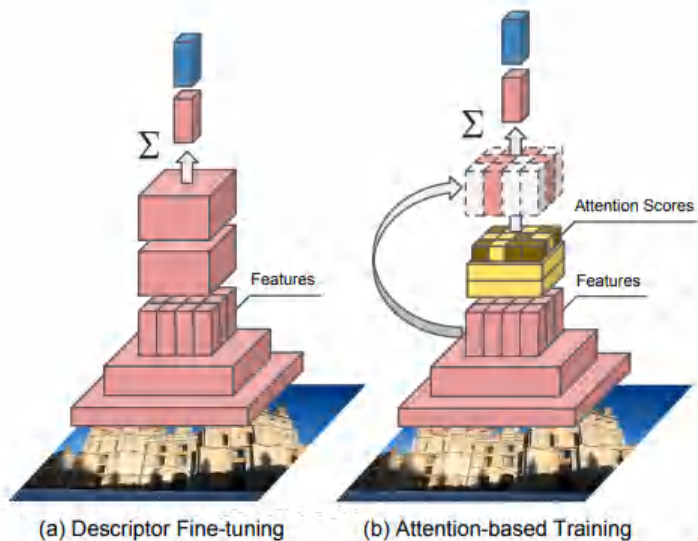


Figure 9: Comparison of keypoint selection methods. (a) Input image (b)  $L_2$  norm scores using the pretrained model (DELF-noFT) (c)  $L_2$  norm scores using fine-tuned descriptors (DELF+FT) (d) Attention-based scores (DELF+FT+ATT). Our attention-based model effectively disregards clutter compared to other options.

“Attention” as weighting  
for global descriptor

# D2Net

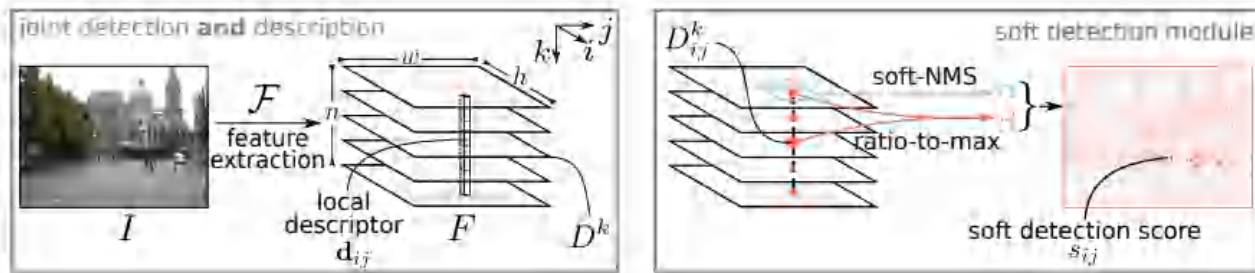


Figure 3: **Proposed detect-and-describe (D2) network.** A feature extraction CNN  $\mathcal{F}$  is used to extract feature maps that play a dual role: (i) local descriptors  $\mathbf{d}_{i,j}$  are simply obtained by traversing all the  $n$  feature maps  $D^k$  at a spatial position  $(i,j)$ ; (ii) detections are obtained by performing a non-local-maximum suppression on a feature map followed by a non-maximum suppression across each descriptor - during training, keypoint detection scores  $s_{i,j}$  are computed from a soft local-maximum score  $\alpha$  and a ratio-to-maximum score per descriptor  $\beta$ .

$$\mathcal{L}(I_1, I_2) = \sum_{c \in \mathcal{C}} \frac{s_c^{(1)} s_c^{(2)}}{\sum_{q \in \mathcal{C}} s_q^{(1)} s_q^{(2)}} m(p(c), n(c)) ,$$

# UR2KiD

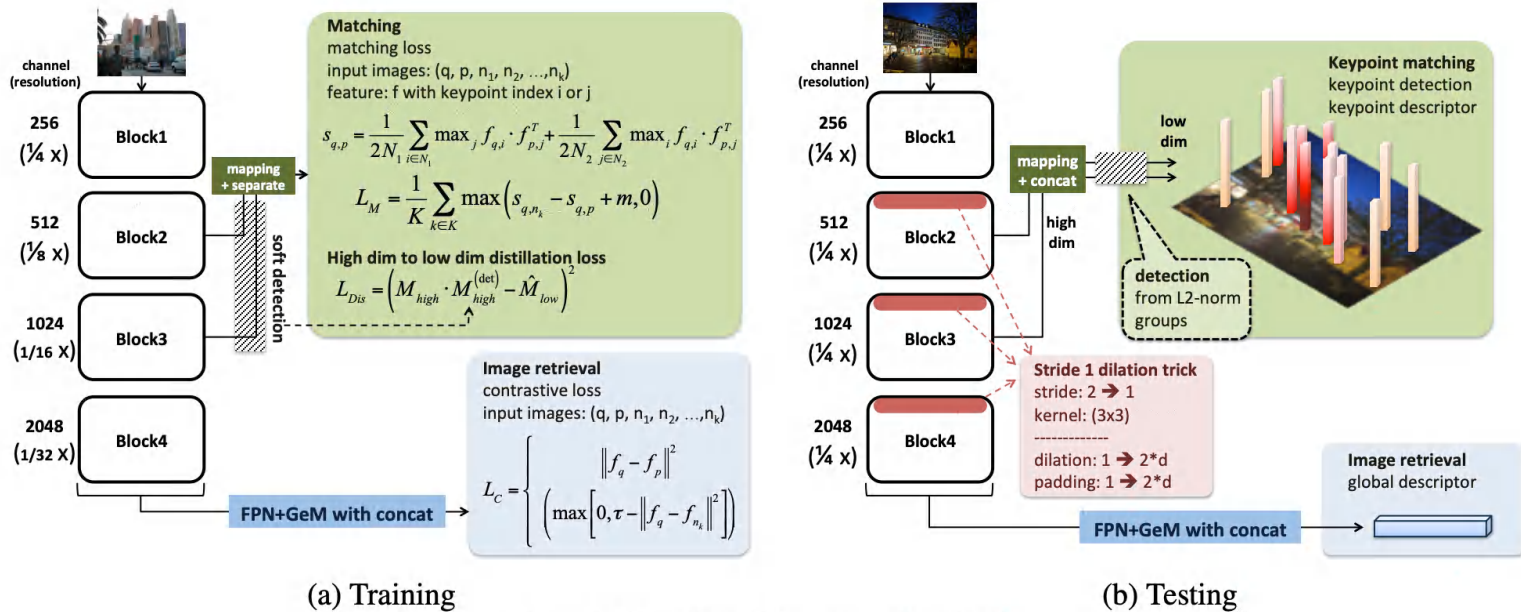
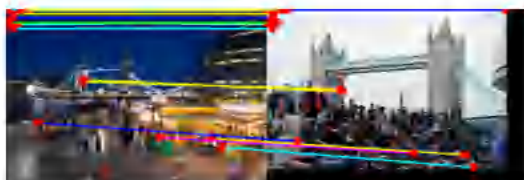
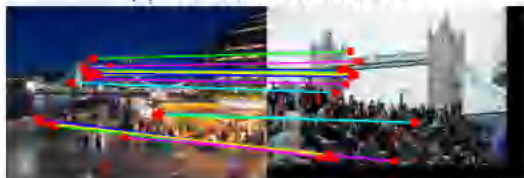


Figure 2. Overview of the proposed method.

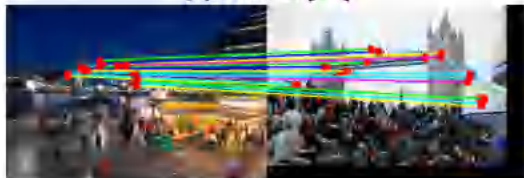
# UR2KiD



(a) Pre-trained ResNet101



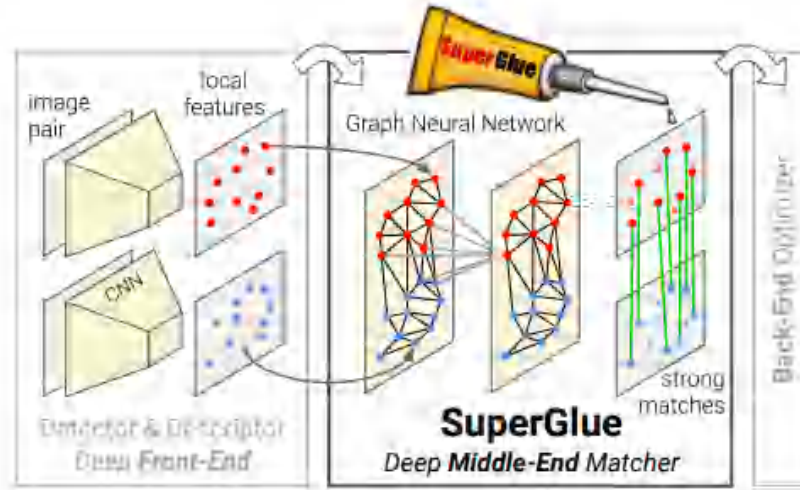
(b) D2-Net [15]



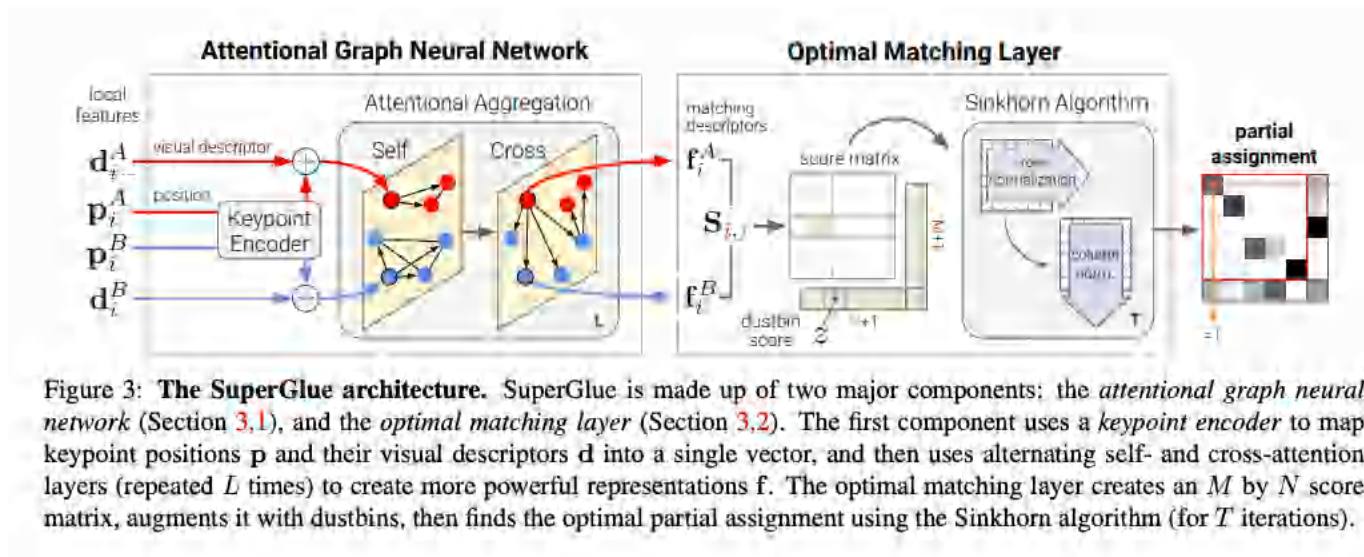
(c) **UR2KiD (ours)**

Figure 1. Extremely challenging image matching scenario with severe scale change and significant scene difference between day and night. The proposed UR2KiD method is able to utilize a common network structure to achieve state-of-the-art results.

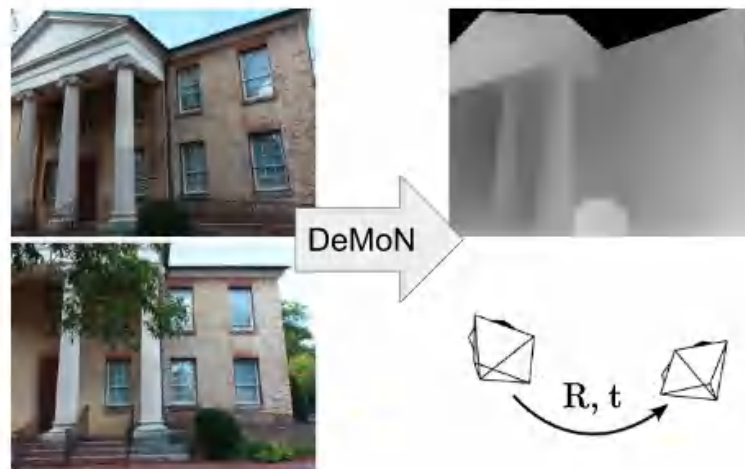
# SuperGlue



# SuperGlue

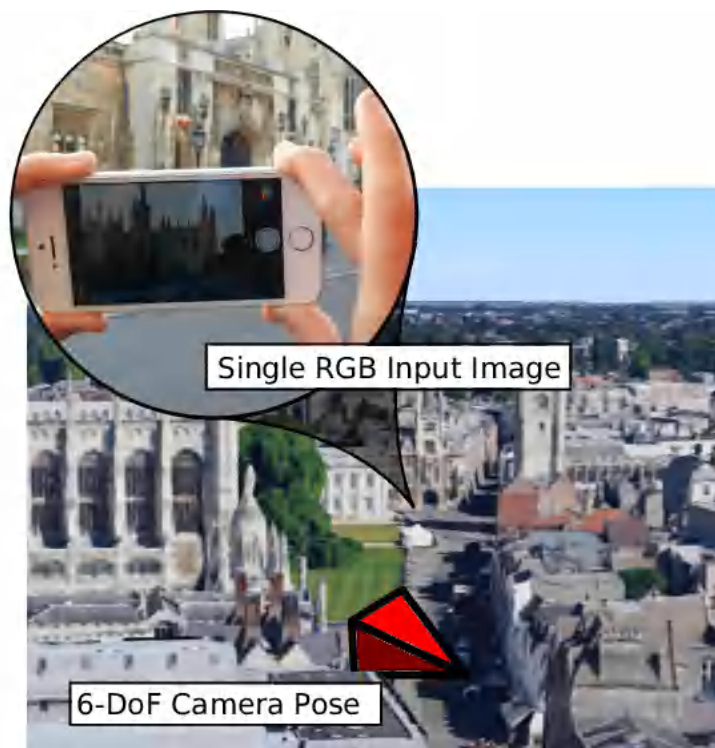


# DeMoN



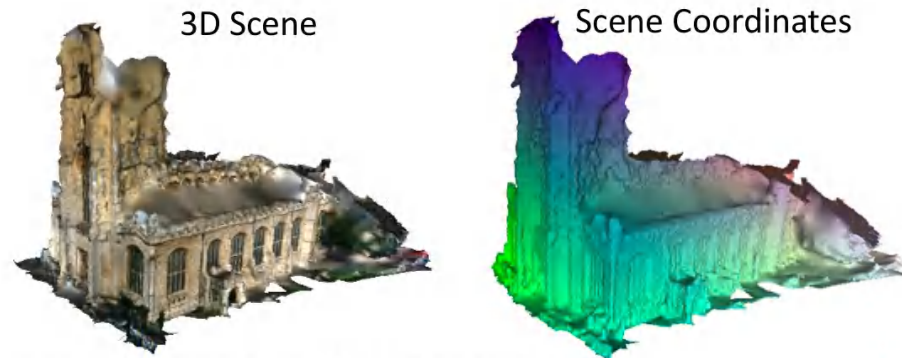


# PoseNet

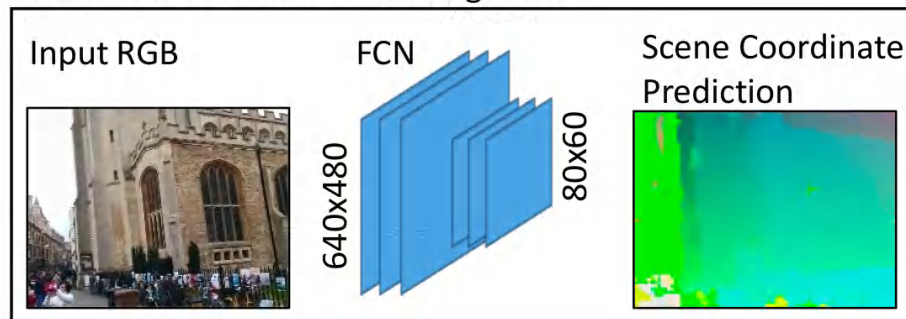




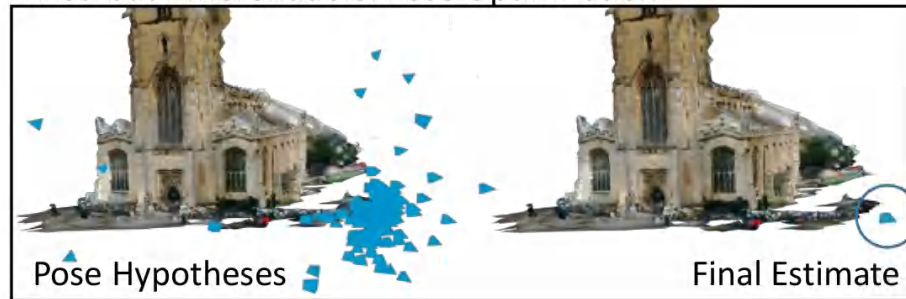
# Local scene coordinates



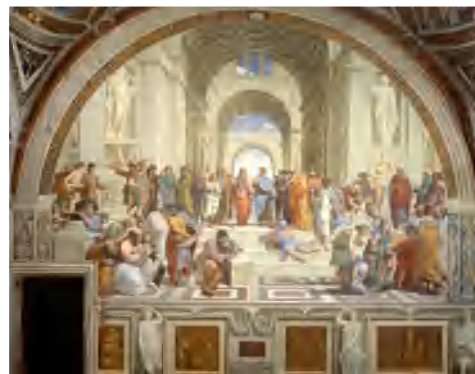
Learned: Scene Coordinate Regression



Fixed but Differentiable: Pose Optimization



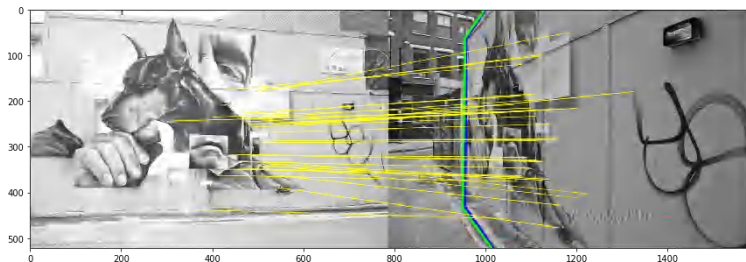
How good are modern methods?



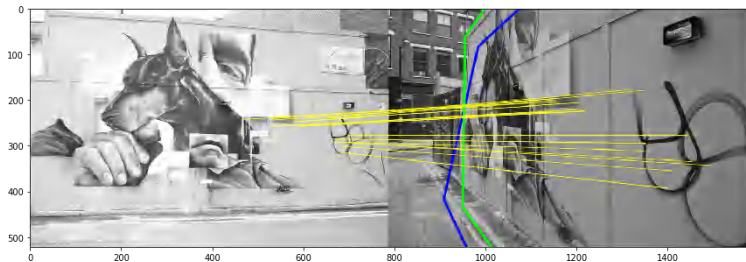




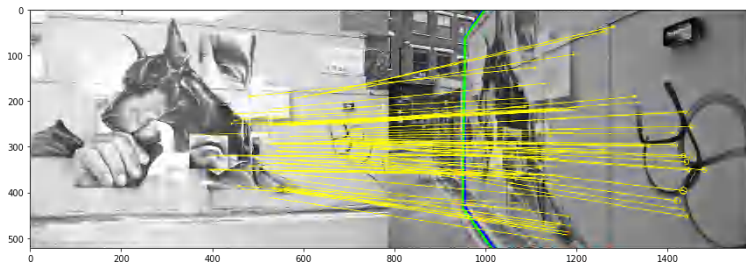
# “Classical” methods are still quite strong



SuperPoint: 51 inliers



D2Net: 26 inliers, incorrect geometry



DoG + HardNet: 123 inliers

More later @ Dmytro's talk!

# State-of-the art & future challenges - open questions

- How can the current matching paradigm be improved?
- Do we still need local features?
- Are dense descriptors using FCN needed?
- Are attention models related to detectors?
- Is end-to-end learning of every stage the best solution?
- How to add semantics into the pipeline?

# Programme

- 09:00 – 10:00 Overview of classical & end-to-end methods
- 10:00 – 11:00 Local features: from paper to practice
- 11:00 – 12:00 Kornia introduction & hands-on Session